Title

Pan-tropical prediction of forest structure from the largest trees

Short Title header

Pan-tropical forest structure from the largest trees

Authors

Jean-François Bastin[1,2,3,4], Ervan Rutishauser[4,5],James R.Kellner[6,7], Sassan Saatchi[8], Raphael Pélissier[9], Bruno Hérault[10,11],Ferry Slik[12], Jan Bogaert[13], Charles De Cannière[2], Andrew R. Marshall[14,15,16], John Poulsen[17], Patricia Alvarez-Loyayza[18], Ana Andrade[19], Albert Angbonga-Basia[20], Alejandro Araujo-Murakami[21], Luzmila Arroyo[22], Narayanan Ayyappan[23,24], Celso Paulo de Azevedo[25], Olaf Banki[26], Nicolas Barbier[9], Jorcely G. Barroso[26], Hans Beeckman[27], Robert Bitariho[28], Pascal Boeckx[29], Katrin Boehning-Gaese[30,31], Hilandia Brandão[32], Francis Q.Brearley[33], Mireille Breuer Ndoundou Hockemba[34], Roel Brienen[35], Jose Luis C.Camargo[19], Sto[36], Benoit Cassart[37,38], Jérôme Chave[39], Robin Chazdon[40], Georges Chuyong[41], David B.Clark[42], Connie J.Clark[17], Richard Condit[43], Euridice N. Honorio Coronado[44], Priya Davidar[22],Thalès de Haulleville[13,27], Laurent Descroix[45],Jean-Louis Doucet[13],Aurelie Dourdain[46],Vincent Droissart[9],Thomas Duncan[47], Javier Silva Espejo[48], Santiago Espinosa[49],Nina Farwig[50],Adeline Fayolle[13], Ted R. Feldpausch[51], Antonio Ferraz[8], Christine Fletcher[36],Krisna Gajapersad[52], Jean-François Gillet[13], Iêda Leão do Amaral[32], Christelle Gonmadje[53], James Grogan[54], David Harris[55],Sebastian K.Herzog[56], Jürgen Homeier[57], Wannes Hubau[27], Stephen P. Hubbell[58,5], Koen Hufkens[29], Johanna Hurtado[59], Narcisse.G.Kamdem[60], Elizabeth Kearsley[61], David Kenfack[62], Michael Kessler[63], Nicolas Labrière[10,64], Yves Laumonier[10,65], Susan Laurance[66], William F.Laurance[66], Simon L. Lewis[35], Moses B. Libalah[60], Gauthier Ligot[13], Jon Lloyd[67,68], Thomas E. Lovejoy[68], Yadvinder Malhi[69], Beatriz S. Marimon[70], Ben Hur Marimon Junior[70], Emmanuel H.Martin[71], Paulus Matius[72], Victoria Meyer[8], Casimero Mendoza Bautista[73], Abel Monteagudo-Mendoza[74], Arafat Mtui[75], David Neill[76], Germaine Alexander Parada Gutierrez[77], Guido Pardo[78],Marc Parren[79], N. Parthasarathy[23],Oliver L. Phillips[35], Nigel C.A. Pitman[79], Pierre Ploton[9],Quentin Ponette[37], B.R.Ramesh[23], Jean-Claude

Razafimahaimodison[80],Maxime Réjou-Méchain[9], Samir Gonçalves Rolim[81], Hugo Romero Saltos[82], Luiz Marcelo Brum Rossi[81], Wilson Roberto Spironello[32], Francesco Rovero[75], Philippe Saner[83], Denise Sasaki[84], Mark Schulze[85], Marcos Silveira[86], James Singh[87], Plinio Sist[10,88], Bonaventure Sonke[60],J.Daniel Soto[89], Cintia Rodrigues de Souza[24], Juliana Stropp[90], Martin J.P. Sullivan[35], Ben Swanepoel[34], Hans ter Steege[25,91],John Terborgh[92,93],Nicolas Texier[94], Takeshi Toma[95], Renato Valencia[96], Luis Valenzuela[74], Leandro Valle Ferreira[97], Fernando Cornejo Valverde[98], Tinde R Van Andel[25],Rodolfo Vasque[76], Hans Verbeeck[61],Pandi Vivek[22],Jason Vleminckx[99], Vincent A.Vos[78,100], Fabien H.Wagner[101], Warsudi[102],Verginia Wortel[103], Roderick J. Zagt[104],Donatien Zebaze[60]

1. Institute of Integrative Biology, Department of Environmental Systems Science, ETH Zürich, 8092 Zürich, Switzerland

2. Landscape Ecology and Plant Production System, Université libre de Bruxelles. CP264-2, B-1050 Bruxelles, Belgium

3. Affiliated during analysis and writing at NASA, Jet Propulsion Laboratory, California Institute of Technology, 4800 Oak Grove Drive, Pasadena, CA 91109, USA

4. Carboforexpert (carboforexpert.ch), 1248 Hermance, Switzerland

5. Smithsonian Tropical Research Institute, Box 0843-03092, Balboa, Ancon, Panama

6. Department of Ecology and Evolutionary Biology, Brown University, Providence, RI 02912, USA

7. Institute at Brown for Environment and Society, Brown University, Providence, RI 02912, USA

8. NASA, Jet Propulsion Laboratory, California Institute of Technology, 4800 Oak Grove Drive, Pasadena, CA 91109, USA

9. AMAP Lab, IRD, CIRAD, CNRS, INRA, Univ. Montpellier, Montpellier, France

10. Cirad, UR Forest & Societies, 34398 Montpellier Cedex 5, France

11. INPHB (Institut National Polytechnique Félix Houphouet Boigny), Yamoussoukro, Ivory Coast

12. Faculty of Science, Universiti Brunei Darusallam, Gadong, BE1410, Brunei Darussalam

13. Gembloux Agro-Bio Tech, Université de Liège, B-5030 Gembloux, Belgium

14. CIRCLE, Environment Department, Wentworth Way, University of York, Heslington, York, YO10 5NG, UK

15. Tropical Forests and People Research Centre, University of the Sunshine Coast, QLD 4556, Australia

16. Flamingo Land Ltd., Kirby Misperton, YO17 6UX, UK

17. Nicholas School of the Environment, Duke University, PO Box 90328, Durham, NC 27708, USA

18. Field Museum of Natural History, Chicago, USA.

19. Biological Dynamics of Forest Fragment Project (BDFFP - INPA/STRI), Manaus - Amazonas, Brazil

20. Institut Facultaire des Sciences Agronomiques de Yangambi. DRC

21. Museo de Historia Natural Noel Kempff Mercado, Santa Cruz, Bolivia

22. Department of Ecology and Environmental Sciences, Pondicherry University, Kalapet, Pondicherry 605014, India

23. French Institute of Pondicherry (IFP), 11 Saint Louis Street, Pondicherry 605 001, India

24. Embrapa Amazônia Ocidental, Brazil

25. Naturalis Biodiversity Centre, PO Box 9517, 2300 RA Leiden, The Netherlands

26. Universidade Federal do Acre, Campus Floresta, Cruzeiro do Sul, Acre, Brazil

27. Service of Wood Biology, Royal Museum for Central Africa, Tervuren, Belgium

28. Institute of Tropical Forest Conservation, Mbarara University of Science and Technology, Uganda.

29. Isotope Bioscience Laboratory – ISOFYS, Ghent University, Belgium

30. Senckenberg Biodiversity and Climate Research Centre (BiK-F), Frankfurt am Main, Germany

31. Dept of Biological Sciences, Goethe Universität, Frankfurt am Main, Germany

32. National Institute for Amazonian Research (INPA), Manaus, Amazonas, Brazil

33. School of Science and the Environment, Manchester Metropolitan University, Chester Street, Manchester, M1 5GD, UK

34. Wildlife Conservation Society, New York, USA

35. School of Geography, University of Leeds, Leeds, UK

36. Malaysia Campus, Jalan Broga, Semenyih 43500, Selangor, Malaysia

37. UCL-ELI, Earth and Life Institute, Université catholique de Louvain, Louvain-la-Neuve BE-1348, Belgium

38. Ecole Régionale Post-universitaire d'Aménagement et de Gestion Intégrés des Forêts et Territoires Tropicaux, Kinshasa, DRC

39. Laboratoire Evolution et Diversité biologique, CNRS & Université Paul Sabatier, Toulouse 31062, France

40. Department of Ecology and Evolutionary Biology, University of Connecticut, Storrs, Connecticut 06268-3043, USA

41. Department of Botany and Plant Physiology, University of Buea, Cameroon

42. Department of Biology, University of Missouri-St Louis, Missouri, USA

43. Field Museum of Natural History and Morton Arboretum, Illinois, USA

44. Coronado, Inst. de Investigaciones de la Amazonia Peruana, Iquitos, Peru

45. ONF pôle R&D, Cayenne, France

46. Cirad, UMR EcoFoG (AgroParisTech, CNRS, Inra, Universite des Antilles, Universite de la Guyane), Kourou, French Guiana

47. Department of Botany and Plant Pathology, Oregon State University, Corvallis, OR 97331, USA

48. Departamento de Biología, Universidad de La Serena, Casilla 554 La Serena, Chile

49. Universidad Autónoma de San Luis Potosí, San Luis Potosí, México

50. Department of Conservation Ecology, Philipps-Universität Marburg, Karl-von-Frisch-Straße 8, 35032 Marburg, Germany

51. Geography, College of Life and Environmental Sciences, University of Exeter, Exeter, EX4 4RJ, UK

52. Conservation International Suriname, Paramaribo, Suriname

53. Department of Plant Biology, Faculty of science, University of Yaounde I, BP 812 Yaoundé, Cameroon

54. Smith College Botanic Garden, Northampton, MA 01063, USA

55. Royal Botanic Garden Edinburgh, Edinburgh EH3 5LR, UK

56. Museo de Historia Natural Alcide d'Orbigny, Cochabamba, Bolivia

57. Plant Ecology, University of Goettingen, Untere Karspuele 2, 37073 Goettingen, Germany

58. Department of Ecology and Evolutionary Biology, University of California, Los Angeles, California 90095, USA

59. Organization for Tropical Studies, Costa Rica

60. Plant Systematic and Ecology Laboratory, Higher Teacher's Training College, University of Yaoundé I, P.O. Box 047, Yaoundé, Cameroon.

61. CAVElab – Computational and Applied Vegetation Ecology, Ghent University, Belgium

62. CTFS-ForestGEO, Smithsonian Tropical Research Institute, MRC 166, NMNH, P.O. Box 37012, Washington, DC 20013-7012, USA

63. Department of Systematic and Evolutionary Botany, University of Zurich, Zollikerstrasse 107, Zurich 8008, Switzerland

64. AgroParisTech, Doctoral School ABIES, 19 Avenue du Maine, 75732 Paris Cedex 15, France

65. Center for International Forestry Research, Jl. CIFOR, Situ Gede, Bogor Barat 16115, Indonesia

66. Centre for Tropical Environmental and Sustainability Science, College of Science and Engineering, James Cook University, Cairns, Queensland 4870, Australia.

67. Department of Life Sciences, Imperial College London, SL5 7PY, Ascot, UK

68. Department of Environmental Science and Policy, George Mason University, Fairfax, VA, USA

69. Environmental Change Institute, School of Geography and the Environment, University of Oxford, Oxford, UK

70. Universidade do Estado de Mato Grosso, Campus de Nova Xavantina, Nova Xavantina, MT, Brazil

71. Udzungwa Ecological Monitoring Centre, Udzungwa Mountains National Park, Tanzania, Sokoine University of Agriculture, Morogoro, Tanzania

72. Faculty of Forestry, Mulawarman University, Indonesia

73. Escuela de Ciencias Forestales, Unidad Académica del Trópico, Universidad Mayor de San Simón, Sacta, Bolivia

74. Jardín Botánico de Missouri, Oxapampa, Pasco, Peru.

75. MUSE - Museo delle Scienze, Trento, Italy

76. Universidad Estatal Amazónica, Puyo, Pastaza, Ecuador

77. Museo de Historia Natural Noel Kempff Mercado, Santa Cruz, Bolivia

78. Universidad Autónoma del Beni, Riberalta, Bolivia

79. Science and Education, The Field Museum, 1400 South Lake Shore Drive, Chicago, Illinois 60605–2496, USA

80. Centre ValBio, Ranomafana, Madagascar

81. Embrapa Florestas, Colombo/PR, Brazil

82. Yachay Tech University, School of Biological Sciences and Engineering. Urcuquí, Ecuador

83. Department of Evolutionary Biology and Environmental Studies, University of Zurich, CH-8057 Zurich, Switzerland

84. Fundação Ecológica Cristalino Alta Floresta, Brazil

85. HJ Andrews Experimental Forest, PO Box 300, Blue River, OR 97413, USA

86. Museu Universitário, Universidade Federal do Acre, Rio Branco 69910-900, Brazil

87. Guyana Forestry Commission, Georgetown, Guyana

88. Forests and Societies, Univ. Montpellier, CIRAD, Montpellier, France

89. Museo de Historia Natural Noel Kempff Mercado, Santa Cruz, Bolivia

90. Institute of Biological and Health Sciences, Federal University of Alagoas, Maceió, Brazil

91. Systems Ecology, Free University, De Boelelaan 1087, Amsterdam, 1081 HV, Netherlands

92. Florida Museum of Natural History and Department of Biology, University of Florida - Gainesville, Gainesville, FL 32611, USA

93. Department of Biology, James Cook University, Cairns, Australia

94. Laboratoire d'Evolution Biologique et Ecologie, Faculté des Sciences, Université libre de Bruxelles, CP160/12, 1050 Bruxelles, Belgium

95. Forestry and Forest Products Research Institute, Matsunosato 1, Tsukuba 305-8687, Japan

96. Escuela de Ciencias Biológicas, Pontificia Universidad Católica del Ecuador, Quito, Ecuador

97. Coordenação de Botânica, Museu Paraense Emilio Goeldi, Belém, Brazil

98. Andes to Amazon Biodiversity Program, Madre de Dios, Peru

99. Department of Integrative Biology, University of California, Berkeley, 1005 Valley Life Sciences Building 3140, Berkeley, CA 94720-3140, USA

100. Centro de Investigación y Promoción del Campesinado - Norte Amazónico, Riberalta, Bolivia

101. Remote Sensing Division, National Institute for Space Research - INPE, São José dos Campos 12227-010, SP, Brazil

191 102. The Center for Reforestation Studies in the Tropical Rain Forest (PUSREHUT),
192 Mulawarman University, Jln. Kihajar Dewantara Kampus Gunung Kelua, Samarinda 75123,
193 East Kalimantan, Indonesia

194 103. Center for Agricultural Research in Suriname (CELOS), Suriname

195 104. Tropenbos International, PO Box 232, Wageningen 6700 AE, The Netherlands

196 **Abstract**

197 **Aim**. Large tropical trees form the interface between ground and airborne observations,
198 offering a unique opportunity to capture forest properties remotely and to investigate their
199 variations on broad scales. However, despite rapid development of metrics to characterize the
200 forest canopy from remotely sensed data, a gap remains between aerial and field inventories.
201 To close this gap, we propose a new pan-tropical model to predict plot-level forest structure
202 properties and biomass from just the largest trees.

203 **Location**. Pan-tropical

204 **Time period**. Early 21st century

205 **Major taxa studied**. Woody plants

206 **Method**. Using a dataset of 867 plots distributed among 118 sites across the tropics, we tested
207 the prediction of the quadratic mean diameter, basal area, Lorey's height, community wood
208 density and aboveground biomass from the ith largest trees.

209 **Result**. Measuring the largest trees in tropical forests enables unbiased predictions of plot and
210 site-level forest structure. The 20 largest trees per hectare predicted quadratic mean diameter,
211 basal area, Lorey's height and community wood density and aboveground biomass with 12%,
212 16%, 4%, 4% and 17.7% of relative error. Most of the remaining error in biomass prediction is
213 driven by differences in the proportion of total biomass held in medium size trees (50-70 cm),
214 which shows some continental dependency with American tropical forests presenting the
215 highest proportion of total biomass in these intermediate diameter classes relative to other
216 continents.

217 **Conclusion**. Our approach provides new information on tropical forest structure and can be
218 employed to accurately generate field estimates of tropical forest carbon stocks to support the
219 calibration and validation of current and forthcoming space missions. It will reduce the cost of
220 field inventories and contribute to scientific understanding of tropical forest ecosystems and
221 response to climate change.

Introduction

The fundamental ecological function of large trees is well established for tropical forests. They offer shelter to multiple organisms (Remm & Lõhmus, 2011; Lindenmayer *et al.*, 2012), regulate forest dynamics, regeneration (Harms *et al.*, 2000; Rutishauser *et al.*, 2010) and total biomass (Stegen *et al.*, 2011), and are important contributors to the global carbon cycle (Meakem *et al.*, 2017). Being major components of the canopy, the largest trees may also suffer more than sub-canopy and understory trees from climate change, as they are directly exposed to variations in solar radiation, wind strength, temperature seasonality and relative air humidity (Laurance *et al.*, 2000; Nepstad *et al.*, 2007; Lindenmayer *et al.*, 2012; Thomas *et al.*, 2013; Bennett *et al.*, 2015; Meakem *et al.*, 2017). Because they are visible from the sky, large trees are ideal for monitoring forest responses to climate change via remote sensing (Bennett *et al.*, 2015; Asner *et al.*, 2017).

Large trees encompass a disproportionate fraction of total aboveground biomass (AGB) in tropical forests (Chave *et al.*, 2001; Lutz *et al.*, 2018), with some variations in their relative contribution to the total AGB among the tropical regions (Feldpausch *et al.*, 2012). In Central Africa, the largest 5% of trees in a forest sample plot, i.e. the 5% of trees with the largest diameter at 130 cm, store 50% of forest plot aboveground biomass on average (Bastin *et al.*, 2015). Consequently, the density of large trees largely explains variation in forest AGB at local (Clark & Clark, 1996), regional (Malhi *et al.*, 2006; Saatchi *et al.*, 2007), and continental scales (Stegen *et al.*, 2011; Slik *et al.*, 2013). Detailing the contribution of each single tree to the diameter structure, we showed previously that plot-level AGB can be predicted from a few large trees (Bastin *et al.*, 2015), with the measurement of the 20 largest trees per hectare being sufficient to estimate plot-level biomass with less than 15% error in reference to ground estimates. These findings suggested that a substantial gain of cost-effectiveness may be achieved by focusing forest inventories on the largest trees rather than all size classes. Similarly, it suggested that remote sensing (RS) approaches could focus on the measurement of the largest trees, instead of properties of the entire forest stand.

Several efforts are underway to close the gap between remote sensing of forest biomass and field surveys (Coomes *et al.*, 2017; Jucker *et al.*, 2017). However, existing RS approaches typically require ground measurement of all trees above or equal to 10 cm of diameter (D) for calibration (Asner *et al.*, 2012; Asner & Mascaro, 2014). Collecting such data in the field is costly and time-consuming, which therefore limits the spatial representativeness of available plot networks. Besides, extrapolation methods of ground-based biomass estimations on RS data still faces important limits. For instance, using mean canopy height extracted from active sensors (Mascaro *et al.*, 2011; Ho Tong Minh *et al.*, 2016), or canopy grain derived from optical images (Proisy *et al.*, 2007; Ploton *et al.*, 2012, 2017; Bastin *et al.*, 2014), the biomass is predicted with an error of only 10-20% compared to ground-based estimates. However, this good level of accuracy is limited to the extent of the RS scene used, which considerably decrease in the upscaling step necessary for national of global maps (Xu *et al.*, 2017). A promising development to alleviate this spatial restriction lies in the 'universal approach', proposed by Asner et al. (2012) and further adapted in Asner and Mascaro (2014), in which plot-level biomass is predicted by a linear combination of ground-based and remotely-sensed metrics. The 'universal approach' relies upon canopy height metrics derived from radar or LiDAR (top of canopy height, TCH), and basal area (BA, i.e. the cumulated cross-sectional stems area) and community wood density (i.e. weighted by basal area, WD_{BA}) derived from field inventories. Plot AGB is then predicted as follows (Asner *et al.*, 2012):

$$AGB = aTCH^{b1}BA^{b2}WD_{BA}^{b3} \quad (1)$$

While generally performing better than approaches based solely on remote sensing of tree height (Coomes *et al.*, 2017), this model relies on exhaustive ground measurements (i.e. wood density and basal area of all trees above 10 cm of diameter at 130 cm, neither of which is measured using any existing remotely sensed data).

Recent advances in remote sensing allow the identification of single trees in the canopy (Ferraz *et al.*, 2016), estimation of adult mortality rates for canopy tree species (Kellner & Hubbell, 2017), description of the forest diameter structure (Stark *et al.*, 2015), depiction of crown and gap shapes (Coomes *et al.*, 2017), and even identification of some functional traits of canopy

277 species (Asner *et al.*, 2017). As routine retrieval of some canopy tree metrics is within reach,
278 we test here the capacity of the largest trees, i.e. trees that can be potentially derived using
279 remote sensing, to predict plot-level biomass. To this end, we adapted equation (1) as follows:
280 $AGB = a(Dg_{LT\,i}H_{LT\,i}WD_{LT\,i})^{b1}$ (2)
281 where for the i^{th} largest trees, Dg_{LT} is the quadratic mean diameter, H_{LT} the mean height, and
282 WD_{LT} the mean wood density among the i^{th} largest trees.
283 Using a large database of forest inventories gathered across the tropics (Figure 1), including
284 secondary and old growth forest plots, we test the ability of the largest trees to predict various
285 metrics estimated at 1-ha plot level, namely the mean quadratic diameter, the basal area, the
286 Lorey's height (i.e. plot-average height weighted by basal area), the community wood density
287 (i.e. plot-average wood density weighted by basal area) and mean aboveground live biomass
288 (supplementary figure 1). By testing different numbers of largest trees as predictors, we aim to
289 propose a threshold of the minimal number of largest trees required to predict forest plot
290 metrics at a pan-tropical level with no bias and low uncertainty (i.e. error inferior to 20%). While
291 previous work focused on estimating biomass in Central African forests (Bastin *et al.*, 2015),
292 the present study aims at generalizing the potential of large trees to predict these different plot
293 metrics at continental and pan-tropical scales. Taking advantage of a unique dataset gathered
294 across the tropics (867 1-ha plots), we also investigate major differences in forest structure
295 across the three main tropical regions: the Americas, Africa and Asia. We further discuss how
296 this approach can be used to guide innovative RS techniques and increase the frequency and
297 representativeness of ground data to support global calibration and validation of current and
298 planned space missions. These include the NASA Global Ecosystem Dynamics Investigation
299 (GEDI), NASA-ISRO Synthetic Aperture Radar (NISAR), and ESA P-band radar (BIOMASS)
300 (Le Toan *et al.*, 2011; Dubayah *et al.*, 2014). This study is a step forward in bringing together
301 remote sensing and field sampling techniques for quantification of terrestrial C stocks in tropical
302 forests.

Material & Methods

Database

For this study, we compiled standard forest inventories conducted in 867 1-ha plots from 118 sites across the three tropical regions (Figure 1), including mature and secondary forests. Each site comprises all the plots in a given geographical location, i.e. within a 10 km radius and collected by a Principal Investigator and its team. These consisted of 389 plots in America (69 sites), 302 plots in Africa (35 sites) and 176 plots in Asia (14 sites). Data were provided by Principal Investigators (see supplementary Table 1), and through datasets available on the following networks: TEAM (http://www.teamnetwork.org/), CTFS (http://www.forestgeo.si.edu/; Condit *et al.*, 2012) and ForestPlots (https://www.forestplots.net/) for AfriTRON (the African Tropical Rainforest Observation Network; www.afritron.org) and RAINFOR (the Amazon forest inventory network; http://www.rainfor.org/) networks.

We selected plots located between 23°N and 23°S, including tropical islands, with an area of 1-ha to ensure stable intra-sample variance in basal area (Clark & Clark, 2000). Plots in which at least 90% of the stems were identified to species, and in which all stems with the diameter at 130 cm greater than or equal to 10 cm had been measured were included. Wood density, here recorded as the wood dry mass divided by its green volume, was assigned to each tree using the lowest available taxonomic level of botanical identifications (i.e. species or genus) and the corresponding average wood density recorded in the Global Wood Density Database (GWDD, Chave *et al.*, 2009; Zanne *et al.*, 2009). Botanical identification was harmonized through the Taxonomic Names Resolution Service (http://tnrs.iplantcollaborative.org), for both plot inventories and the GWDD. For trees not identified to species or genus (~5%), we used plot-average wood density. We estimated heights of all trees using Chave et al.'s (2014) pan-tropical diameter-height model which accounts for heterogeneity in the D-H relationship using an environmental proxy:

$$\ln(H) = 0.893 - E + 0.760 \ln(D) - 0.0340 \ln(D)^2 \quad (3)$$

Where D is the diameter at 130 cm and E is a measure of environmental stress (Chave *et al.*, 2014). For sites with tree height measurements (N=20), we developed local D-H models, using

a Michaelis-Menten function (Molto *et al.*, 2014). We used these local models to validate the predicted Lorey's height (i.e. plot average height weighted by BA) from the largest trees, of which height has been estimated with a generic H-D model (equation 3, Chave et al. 2014). We estimated plot biomass as the sum of the biomass of live tree with diameter at 130 cm superior or equal to 10 cm, using the following pan-tropical allometric model (Réjou-Méchain *et al.*, 2017):

$$AGB=\exp(-2.024-0.896E+0.920\ln(WD)+2.795\ln(D)-0.0461(\ln(D^2))) \quad (4)$$

Plot-level metric estimation from the largest trees

The relationship between each plot metric, namely basal area (BA), the quadratic mean diameter (Dg), Lorey's height ($H_{BA;}$ the mean height weighted by the basal area) and the community wood density (WD_{BA}; the mean wood density weighted by the basal area), and those derived from largest trees was determined using an iterative procedure following Bastin et al. (2015). Trees were first ranked by decreasing diameter in each plot. An incremental procedure (i.e. including a new tree at each step) was used to sum or average information of the *i* largest trees for each plot metric. Each plot-level metric was predicted by the respective metric derived from the i^{th} largest trees. For each increment, the ability (goodness of fit) of the *i* largest trees to predict a given plot-metric was tested through a linear regression. To avoid overfitting, a Leave-One-Out procedure was used to develop independent site-specific models (N=118). Specifically, the model to be tested at a site was developed with data from all other sites. Errors were then estimated as the relative root mean square error (rRMSE) computed between observed and predicted values (X):

$$rRMSE = \sqrt{\sum \frac{(Xobs - Xpred)^2}{n}} / \bar{X} \quad (5)$$

The form of the regression model (i.e. linear, exponential) was selected to ensure a normal distribution of the residuals.

To estimate plot basal area, we used a simple power-law constrained on the origin, as linear model resulted in non-normal residuals. Plot-level basal area (BA) was related to the basal area for the *i* largest trees (BA_i) using:

$BA = b_1 \Sigma BA_i^{\gamma 1}$ (6)

To estimate the quadratic mean diameter, Lorey's height and the wood density of the community, we used simple linear models relating the plot-level metrics and the value of the metrics for the *i* largest trees:

$D_g = a_2 + b_2 D_{gi}$ (7)

$H_{BA} = a_3 + b_3 \overline{H_i}$ (8)

$WD_{BA} = a_4 + b_4 \overline{WD_i}$ (9)

Both Lorey's height (H_{BA}) and the average height ($\overline{H_i}$) of the i^{th} largest trees depend on the same D-H allometry, which always contains uncertainty whether we use a local, a continental or a pan-tropical model. To test the dependence of the prediction of H_{BA} from $\overline{H_i}$ on the allometric model, we used measurement from Malebo in the Democratic Republic of the Congo, where all heights were measured on the ground (see supplementary figure 2).

The quality of the predictions of plot-level metrics from the largest trees is quantified using the relative root mean square error (rRMSE) between measured and predicted values, and displayed along the cumulated number of largest trees. Model coefficients are estimated for each metric derived from the largest trees (N_{LT}) and averaged across the 118 models (see supplementary table 2).

Mean rRMSE is plotted as a continuous variable, while its variation is presented as a continuous area between 5^{th} and the 95^{th} percentiles of observed rRMSE.

The optimal number of largest trees for plot-level biomass estimation

The optimal number of largest trees N_{LT} was determined from the prediction of each plot-level metric considered above, i.e. keeping a small number of trees while ensuring a low level of error for each structural parameter. We then predicted plot-level biomass from the N_{LT} model (equation 2). The final error was calculated by propagating the entire set of errors related to equation 4 (Réjou-Méchain *et al.*, 2017) in the N_{LT} model (i.e. error associated to each allometric model used). The model was then cross-validated across all plots (N=867).

384 **Investigating residuals: what the largest trees do not explain**

385 To understand the limits of predicting AGB through N_{LT}, we further investigated the relationship
386 between AGB residuals and key structural and environmental variables using linear modelling.
387 Forest structure was investigated through the total stem density (N), the quadratic mean
388 diameter (Dg), Lorey's height (H_{BA}) and community wood density (WB_{BA}). As environmental
389 data, we used the mean annual rainfall and the mean temperature computed over the last 10
390 years at each site using the Climate Research Unit data (New *et al.*, 1999, 2002), along with
391 rough information on soil types (Carré *et al.*, 2010). Major soil types were computed from the
392 soil classification of the Harmonized World Soil Database into IPCC (intergovernmental panel
393 on climate change) soil classes. In addition, considering observed differences in forest
394 structure across tropical continents (Feldpausch *et al.*, 2011, 2012) and recent results on pan-
395 tropical floristic affinities (Slik *et al.*, 2015), we tested for an effect of continent (America, Africa
396 and Asia) on the AGB residuals. Differences in forest structure and AGB among continents
397 were also illustrated through the analysis of their distribution.

398 The importance of each variable was evaluated by calculating the type II sum of squares that
399 measures the decrease in residual sum of squares due to an added variable once all the other
400 variables have been introduced into the model (Langsrud, 2003). Residuals were investigated
401 at both plot and site levels, the latter analyzed to test for any influence of the diameter structure,
402 which is usually unstable at the plot level due to the dominance of large trees on forest metrics
403 at small scales (Clark & Clark, 2000). Here we use a principal component analysis (PCA) to
404 summarize the information held in the diameter structure by ordinating the sites along the
405 abundance of trees in each diameter class (from 10 to +100 cm by 10 cm bins).
406

Results

Plot-level metrics

Plot metrics averaged at the site level (867 plots, 118 sites) present important variations within and between continents. In our database, the quadratic mean diameter varies from 15 to 42 cm^2ha^{-1}, the basal area from 2 to 58 m^2ha-1, Lorey's height from 11 to 33 m and the wood density weighted by the basal area from 0.48 to 0.84 gcm^{-3} (supplementary figure 1). Such important differences between minimal and maximal values are observed because our database cover sites with various forest types, from young forest colonizing savannas to old growth forest. However, most of our sites are found in mature forests, as shown by relatively high average and median value of each plot metric (average aboveground biomass = 302 $Mgha^{-1}$; supplementary figure 1). In general, highest values of aboveground biomass are found in Africa, driven by highest values of basal area and highest estimations of Lorey's height. Highest values of wood density weighted by basal area are found in America.

Plot-level estimation from the i largest trees

Overall, plot metrics at 1-ha scale were well predicted by the largest trees, with qualitative agreement among global and continental models (Figure 2). When using the 20 largest trees to predict basal area (BA) and quadratic mean diameter (Dg), the mean rRMSE was < 16% and 12%, respectively (Figs 3a and 3b). Lorey's height (H_{BA}) and wood density weighted by basal area (WD_{BA}) were even better predicted (Figs 3c and 3d), with mean rRMSE of 4% for the 20 largest trees. The prediction of Lorey's height from the largest trees using local diameter-height model (supplementary figure 2a) yielded results similar to those obtained using equation 3 of Chave et al. (2014). More importantly, it also yielded similar results to prediction of Lorey's height from the largest trees using plots where all the trees were measured on the ground (supplementary figure 2b). This suggests that our conclusions are robust to the uncertainty introduced by height-diameter allometric models.

AGB prediction from the largest trees

We selected "20" as the number of largest trees to predict plot metrics. The resulting model predicting AGB (Mg ha^{-1}) based on the 20 largest trees is:

435 $AGB = 0.0735 \times (Dg_{20}H_{20}WD_{20})^{1.1332}$ (rRMSE=0.179; R^2=0.85; AIC= -260.18) (10)

436 Because the exponent was close to 1, we also developed an alternative and more operationa

437 l model with the exponent constrained to 1, given by:

438 $AGB = 0.195 \times (Dg_{20}H_{20}WD_{20})$ (rRMSE=0.177; R^2=0.85; AIC=-195) (11)

439 Ground measurements of plot AGB were predicted by our N_{LT} model with the exponent

440 constrained to 1, with a total error of 17.9% (Figure 4), a value which encompass the error of

441 the N_{LT} model and the error related to the allometric model chosen. The Leave-One-Out cross-

442 validation procedure yielded similar results (rRMSE=0.19; R^2=0.81), validating the use of the

443 model on independent sites.

444 **Determining the cause of residual variations**

445 The explanatory variables all together explain about 37% of the variance in AGB both at plot

446 and site levels when omitting the diameter structure, and about 63% at site level when included

447 (Figure 5). In general, forest structure and particularly the stem density explained most of the

448 residuals (table 1; weights: 79% and 54% at plot- and site-level respectively). The stem density

449 was followed by a continental effect (weights: 18%, 28% and 1%, respectively for Africa,

450 America and Asia) and by the effect of H_{BA} and WD_{BA} (respective weights: 1% and 0% at the

451 plot level, 0% and 11% at the site level, and 23% and 0% when accounting for the diameter

452 structure at the site level). Inclusion of the diameter structure provided the best explanation of

453 residuals, with 63% of variance explained, and a weight of 69% for the first axis of the PCA

454 (supplementary figure 3). This first axis of the PCA was related to the general abundance of

455 trees at a site, and in particular medium-sized trees (40-60cm). Among environmental

456 variables, only rainfall was significantly related to the residuals at the site level when the

457 diameter structure was considered (2%).

458 **Differences among continents**

459 While diameter structure explained a large fraction of the residual variance of our global model,

460 there was marked difference in forest structure across continents (Figure 6). Consequently,

461 we investigated differences between continents in the distribution of residuals of the pan-

462 tropical model (Figure 6a), in the relative contribution of the 20 largest trees to plot total

463 biomass (Figure 6b), and in the contribution to the total aboveground biomass per diameter
464 class (Figs. 6c-f). To this end, we considered the following four classes of diameter at 130 cm:
465 10 to 30 cm, 30 to 50 cm, 50 to 70 cm and above 70 cm. Results show that the prediction of
466 biomass from the 20 largest trees using the pan-tropical model tends to be slightly
467 overestimated in Africa (+ 3%) and underestimated in America (- 3%) and in Asia (-5%) (Figure
468 6a). The proportion of biomass is higher in high diameter class (over 70 cm) in Africa, in
469 intermediate diameter classes (between 30 and 70 cm) in America and is equally distributed
470 among the different diameter classes in Asia (Figure 6 c-d).

Discussion

The largest trees, convergences and divergences between continents

Sampling a few largest trees per hectare generally allows an unbiased prediction of four key descriptors of forest structures across the tropics. There is generally no improvement in predicting biomass, quadratic mean diameter, Lorey's height (H_{BA}) or community wood density beyond the first 10-to-20 largest trees (Figure 2, Figure 3a). But when a forest plot presents an abundant number of large trees (Figure 5d), increasing the number of trees sampled does improve the model's accuracy. This is due to the fact that the higher total AGB in a plot, the lower the proportion of total AGB encompassed by the largest trees. This is particularly true for BA for which rRMSE continues to decrease up to 100 largest trees (Figure 2a). In contrast, Lorey's height predictions are altered when a large number of trees are included (Figure 2c), i.e. when smaller, often suppressed, trees draw the average down (Farrior et al., 2016). This might explain why the prediction of AGB does not mirror that of basal area (Figure 2b, Figure 3a), and suggest that the number of largest trees shall be set independently to each predictor considered. Interestingly, the evolution of relative error in AGB prediction as a function of the number of largest trees considered does not follow the same path between continents. For instance, the error of prediction saturates more quickly in Africa and Asia than America. Investigation of residuals showed that the diameter structure (Figure 5c, supplementary Figure 3b), and in particular the number of medium size trees (Figure 5d), drives variability in AGB predictions. It is therefore not surprising to see that in our dataset the site with higher levels of underestimations is the one with the highest number of medium size trees, which is found in Asia in the Western Ghats of India.

The good performance of models based on the 20 largest trees in predicting Lorey's height and community wood density at site level was not surprising. Both metrics were indeed weighted by basal area, driven de facto by the largest trees. Their consistency across sites and continents was not expected though, which emphasize the generality of our approach.

The predictability of plot-level forest structure metrics from the largest trees implies that characteristics of smaller trees do not vary completely independently from those of the larger

trees. For example, plots where the largest trees have low basal area tend to have low plot-level basal area (Figure 3a), meaning that the total size of the smaller trees is sufficiently constrained so that it does not compensate for the small size of the largest trees. Such constraints could arise through size-frequency distributions being set by allometric scaling rules (Enquist et al., 2009), or could be due to the largest trees responding in the same way as the remaining smaller trees to environmental drivers.

Despite the general consistency of these relationships across continents, slight differences are evident when comparing the pan-tropical model residuals across continents (Figure 6, supplementary figure 4). These differences indicate biogeographic variation in forest structure. In America, our pan-tropical model tends to slightly underestimate basal area (mean: -5%) and overestimate Lorey's height (mean: +3%) (supplementary figure 4). This suggests that large trees make up a smaller proportion of basal area in America and that for a given diameter we find higher trees (supplementary figure 2), the later confirming that the shape of height-diameter allometries varies between continents (Banin et al., 2012; Sullivan et al., 2018). In Africa, large trees (i.e. DBH > 70 cm) are more abundant and account for a large fraction of plot biomass (figure 6f). This supports previous observations that African forests are characterized by fewer but larger stems (Feldpausch *et al.*, 2012; Lewis *et al.*, 2013), while forests in the Americas have more stems but generally have lower biomass (Sullivan et al., 2017). In Asia, the distribution of the biomass across diameter classes appears more balanced (Figure 6c-f). Such differences in forest structure, even if being quite limited, suggest tropical forests differ between continents in terms of dynamics, carbon cycling, response and feedback to climate and resilience to external forcings (e.g. climate change, forest degradation and deforestation).

Interestingly, while a recent global phylogenetic classification of tropical forest groups American with African forests vs. Asian forests (Slik et al., 2018), our study of forest structure properties tends more to single out American forests, and particularly highlight the contrast in between African and American forests. Although this deserves further investigations, it might reveal a lack of close relationship between forest structure properties and phylogenic similarity,

which echoes recent results on the absence of relationship between tropical forest diversity and biomass (Sullivan et al., 2017).

Largest trees, a gateway to global monitoring of tropical forests

Revealing the predictive capacity held by the largest trees, our results constitute a major step forward to monitor forest structures and biomass stocks. The largest trees in tropical forests can therefore be used to accurately predict various ground-measured properties (i.e. the quadratic mean diameter, the basal area, Lorey's height and community wood density), while previous work has predicted only biomass "estimates" (e.g. Slik *et al.*, 2013; Bastin *et al.*, 2015). Our approach allows us to (i) describe forest structure independently of any biomass allometric model (ii) and integrates environmental-based variations in D-H relationship, known to vary locally (Feldpausch *et al.*, 2011; Kearsley *et al.*, 2013;). It is also (iii) relatively insensitive to differences in floristic composition and community wood density (Poorter *et al.*, 2015).

Furthermore, the "largest trees" models were developed for each plot-level metric and for any number of largest trees. Thus, they do not rely on any arbitrary threshold of tree diameter. Note that the optimal number of largest trees to be measured (i.e. 20) was set for demonstration and can vary depending on the needs and capacities of each country or project (see supplementary table 2). In the same way, local models could integrate locally-developed biomass models, when available. Consequently our approach (i) can be used in young or regenerating un-managed forests with a low "largest tree" diameter threshold and (ii) is compatible with recent remote sensing approaches able to single out canopy trees and describe their crown and height metrics (Ferraz *et al.*, 2016; Coomes *et al.*, 2017).

Aboveground biomass model from the largest trees, a multiple opportunity

Globally, the N_{LT} model for the 20 largest trees allows plot biomass to be predicted with 17.9% error. This result is a pan-tropical validation of results obtained in Central Africa (Bastin *et al.*, 2015). It opens new perspectives towards cost-effective methods to monitor forest structures and carbon stocks through largest trees metrics, i.e. metrics of objects directly intercepted by remote-sensing products.

555 Developing countries willing to implement Reduction of Emissions from Deforestation and
556 Forest Degradation (REDD+) activities, shall also report on their carbon emissions and develop
557 a national reference level (IPCC, 2006; Maniatis & Mollicone, 2010). However, most tropical
558 countries lack capacities to assume multiple, exhaustive and costly forest carbon inventories
559 (Romijn *et al.*, 2012). By measuring only a few large trees per hectare, our results show that it
560 is possible to obtain unbiased estimates of aboveground C stocks in a time and cost-efficient
561 manner. Assuming that 400 to 600 trees D > 10 cm are measured in a typical 1-ha sample
562 plot, monitoring only 20 trees is a significant improvement. Although finding the 20 largest trees
563 in a plot of several hundred individuals requires evaluating more than 20 trees, in practice, a
564 conservative diameter threshold could be defined to ensure that the 20 largest trees are
565 sampled. An alternative approach could also be found in the development of relascope-based
566 approach adapted to detection of the largest trees in tropical forests. Using such approach
567 would facilitate rapid field sampling in extensive areas to produce large scale AGB estimates.
568 Those could fulfil the needs in calibration and validation of current and forthcoming space
569 missions focused on aboveground biomass.
570 Our findings also point towards the potential effectiveness of using remote sensing techniques
571 to characterize canopy trees for inferring entire forest stands attributes. Remote sensing data
572 could be used for direct measurement (e.g. tree level metrics such as height, crown width,
573 crown height) of the largest trees as a potential alternative to indirect development of complex
574 metrics (e.g. mean canopy height, texture) used to extrapolate forest properties. While the use
575 of single-tree approach has shown some limitations to extrapolate plot metrics (Coomes *et al.*,
576 2018), we have still to investigate their potential to identify largest trees. Some further
577 refinements are needed, but most of the tools required to develop “largest trees” models are
578 readily available. In particular, Ferraz et al. (2016) developed an automated procedure to locate
579 single trees based on airborne LiDAR data, to measure their height and crown area. Crown
580 area could further be linked to basal area, as the logarithm of crown area is consistently
581 correlated with a slope of 1.2-1.3 to the logarithm of tree diameter across the tropics (Blanchard
582 *et al.*, 2016). Regarding wood density, hyperspectral signature and high resolution topography

583 offers a promising way to assess functional traits remotely (e.g. Asner *et al.*, 2017; Jucker *et*
584 *al.*, 2018) which could potentially provide proxies of wood density. Alternative approaches
585 could focus on the development of plot-level AGB prediction by replacing the basal area of the
586 largest trees with their crown metrics. While the measurement of crown areas has yet to be
587 generalized when inventorying plots, several biomass allometric models already partition trunk
588 and crown mass (Ploton *et al.*, 2016; Coomes *et al.*, 2017; Jucker *et al.*, 2017).
589 The main limitation of our approach lies in the limited inference that can be made on the
590 understory and sub-canopy trees. We show that most of the remaining variance is explained
591 by variations in diameter structures, and in particular among the total stem density.
592 Interestingly, stem density was generally identified as a poor predictor of plot biomass in
593 tropical forests (Slik *et al.*, 2010; Lewis *et al.*, 2013). However, our results show that stem
594 density explains most of the remaining variance (Table S1). This suggests that, in addition to
595 trying to understand large-scale variations in large trees and other plot metrics, which can be
596 directly quantified from remote sensing, we should also put more effort into understanding
597 variation in smaller trees, which mainly drives total stem density and the total floristic diversity.
598 Smaller trees are also essential to characterize forest dynamics and understand changes in
599 carbon stocks. Several options are nonetheless possible from remote sensing, considering the
600 variation in lidar point density below the canopy layer (D'Oliveira *et al.*, 2012), the distribution
601 of leaf area density (Stark *et al.*, 2012, 2015; Tang & Dubayah, 2017; Vincent *et al.*, 2017) or
602 the use of multitemporal lidar data to get information on forest gap generation dynamics and
603 consequently on forest diameter structure (Kellner *et al.*, 2009; Farrior *et al.*, 2016).
604 **Large trees in degraded forests**
605 If large trees are a key feature of unmanaged forests, they are conspicuously absent from
606 managed or degraded forests. Indeed, large trees are targeted by selective or illegal logging,
607 and are the first to disappear or to suffer from incidental damages when tropical forests are
608 exploited for timber (Sist *et al.*, 2014). The loss of largest trees drastically changes forest
609 structures and diameter distributions, and their loss is likely to counteract the consistency in
610 forest structures observed through this study. Understanding how, or whether, managed

611 forests deviate from our model predictions could help characterize forest degradation, which
612 accounts for a large fraction of carbon loss worldwide (Baccini *et al.*, 2017), acknowledging
613 that rapid post-disturbance biomass recovery (Rutishauser *et al.*, 2015) will remain hard to
614 capture.

615 **Conclusion – towards improved estimates of tropical forest biomass**

616 The acquisition, accessibility and processing capabilities of very high spatial, spectral and
617 temporal resolution remote sensing data has increased exponentially in recent years (Bastin
618 *et al.*, 2017). However, to develop accurate global maps, we will have to obtain a greater
619 number of field plots and develop new ways to use remote sensing data. Our results provide
620 a step forward for both by (i) drastically decreasing the number of individual tree measurements
621 required to get an accurate, yet less precise, estimate of plot biomass and (ii) opening the way
622 to direct measurement of plot metrics measured from remote sensing to estimate plot biomass.
623 As highlighted by Clark and Kellner (2012), new biomass allometric models relating plot-level
624 biomass measured from destructive sampling and plot-level metric measured from remote-
625 sensing products should be developed, as an alternative to current tree-level allometric
626 models. Such an effort will largely lower operational costs and uncertainties surrounding
627 terrestrial C estimates, and consequently, will help developing countries in the development of
628 national forest inventories and aid the scientific community in better understanding the effect
629 of climate change on forest ecosystems.

630 **Acknowledgments**

631 J.-F.B. was supported for data collection by the FRIA (FNRS), ERAIFT (WBI), WWF and by
632 the CoForTips project (ANR-12-EBID-0002); T.d.H. was supported by the COBIMFO project
633 (Congo Basin integrated monitoring for forest carbon mitigation and biodiversity) funded by the
634 Belgian Science Policy Office (Belspo); C.H.G was supported by the “Sud Expert Plantes”
635 project of French Foreign Affairs, CIRAD and SCAC. Part of data in this paper was provided
636 by the RAINFOR Network, the AfriTRON network, TEAM Network, the partnership between
637 Conservation International, The Missouri Botanical Garden, The Smithsonian Institution and
638 The Wildlife Conservation Society, and these institutions and the Gordon and Betty Moore

Foundation. This is [number to be completed] publication of the technical series of the Biological Dynamics of Forest Fragment Project (INPA/STRI). We acknowledge data contributions from the TEAM network not listed as co-authors (upon voluntary basis). We thank Jean-Phillipe Puyravaud, Estação Científica Ferreira Penna (MPEG) and the Andrew Mellon Foundation and National Science Foundation (DEB 0742830). The forest plots in Nova Xavantina and Southern Amazonia, Brazil was funded by grants from Project PELD-CNPq/FAPEMAT (403725/2012-7; 441244/2016-5; 164131/2013); CNPq-PPBio (457602/2012-0); productivity grants (CNPq/PQ-2) to B. H. Marimon-Junior and B. S. Marimon; Project USA-NAS/PEER (#PGA-2000005316) and Project ReFlor FAPEMAT 0589267/2016. And finally, we thank Helen Muller-Landau for her careful revision and comments of the manuscript.

Contributions

J.F.Bastin and E.Rutishauser conceptualized the study, gathered the data, performed the analysis and wrote the manuscript. All the co-authors contributed by sharing data and reviewing the main text. A.R.Marshall, J.Poulsen and J.Kellner revised the English.

Conflict of interest

The authors declare there is no conflict of interest associated to this study.

Figures

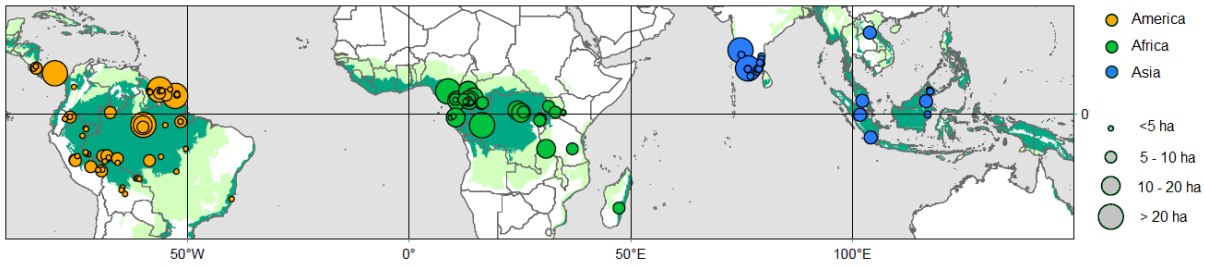

Figure 1. Geographic distribution of the plot database. We used 867 plots of 1 hectare from 118 sites. Dots are colored according to floristic affinities (Slik et al. 2015), with America, Africa and Asia respectively in orange, green and blue. They are also sized according the total area surveyed in each site. In the background, moist forests are displayed in dark green and dry forest in light green.

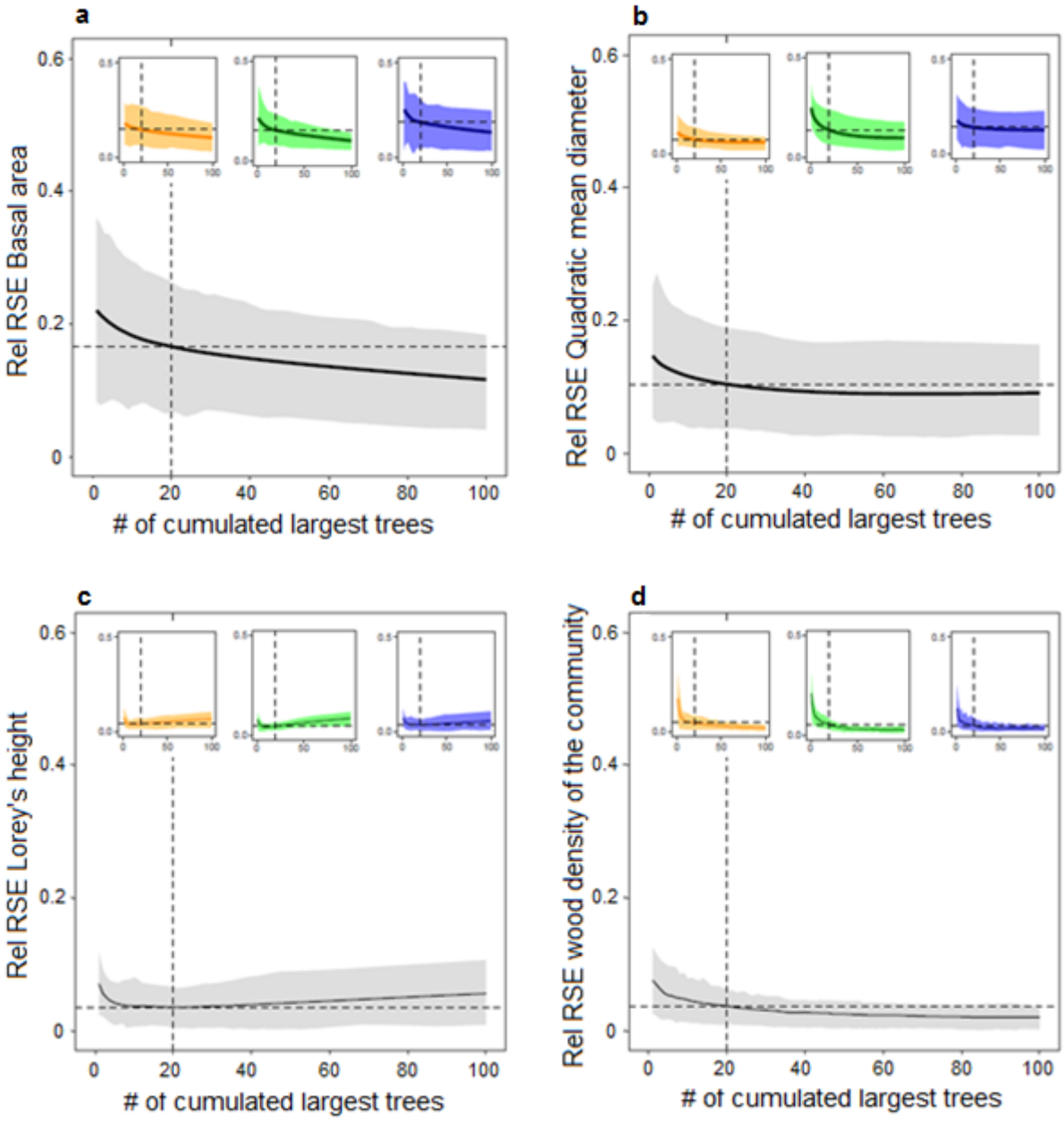

Figure 2. Quality of the prediction of plot metrics from largest trees. Variation of the relative Root Mean Square Error (rRMSE) of the prediction of plot metric from i largest trees versus the cumulative number of largest trees for (a) basal area, (b) quadratic mean diameter, (c) Lorey's height and (d) wood density weighted by the basal area. Results are displayed at the pan-tropical level (main plot in grey) and at the continental level (subplots; orange = America; green = Africa; blue = Asia). The solid line and shading shows the mean rRMSE and the 5th and the 95th percentiles. Dashed lines represent the mean rRMSE observed for each model, when considering the 20 largest trees.

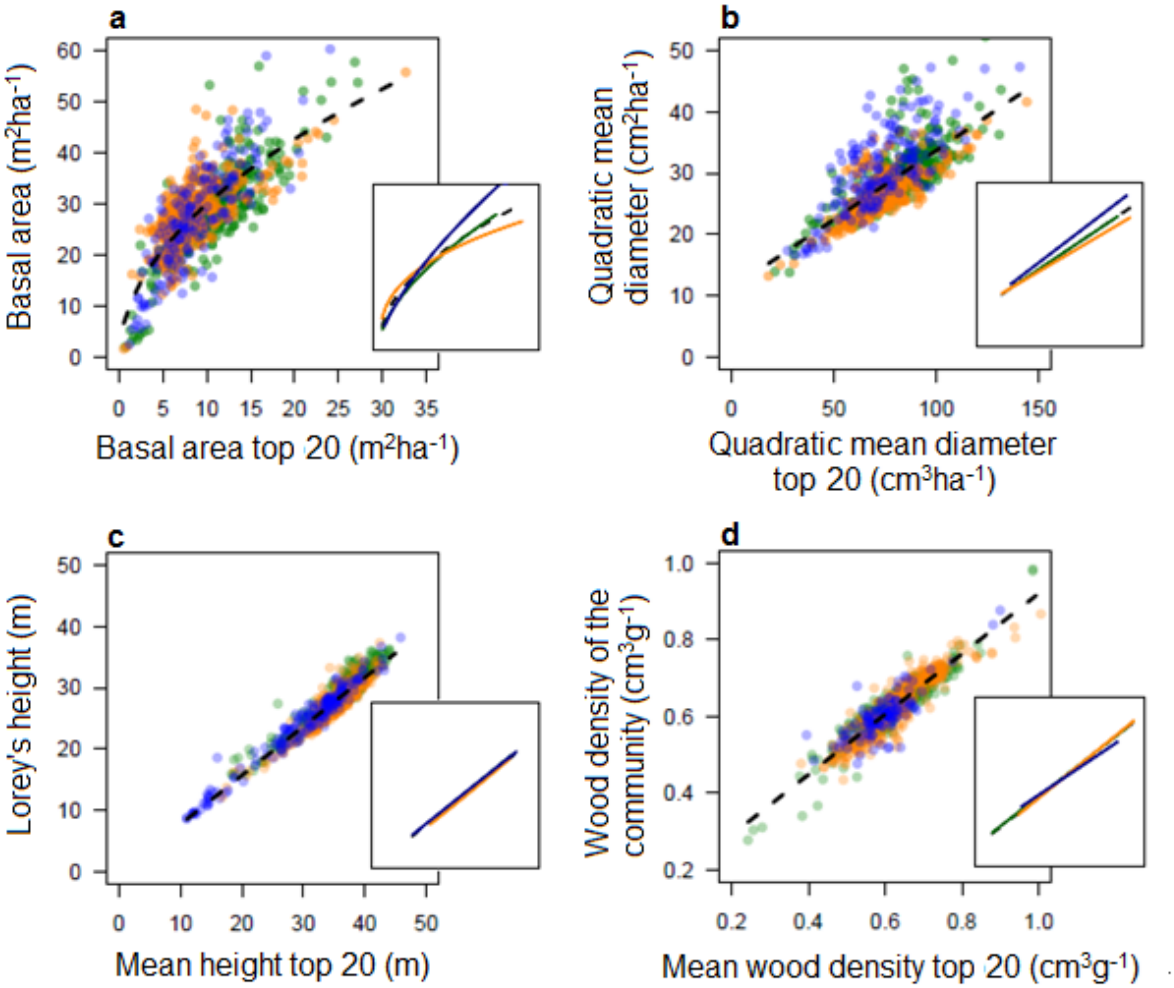

672

673 **Figure 3. Prediction of plot metrics (y-axis) from the 20 largest trees (x-axis).** Results are
674 shown for (a) basal area, (b) quadratic mean diameter, (c) Lorey's Height and (d) wood density
675 weighted by the basal area. Each dot corresponds to a single plot, colored in orange, green
676 and blue for America, Africa and Asia respectively. Both pan-tropical (black dashed lines) and
677 continental (coloured lines) regression models are displayed. These results show that
678 substantial part of remaining variance, i.e. not explained by largest trees, is found when
679 predicting the basal area and the quadratic mean diameter, with slight but significant
680 differences between continents.

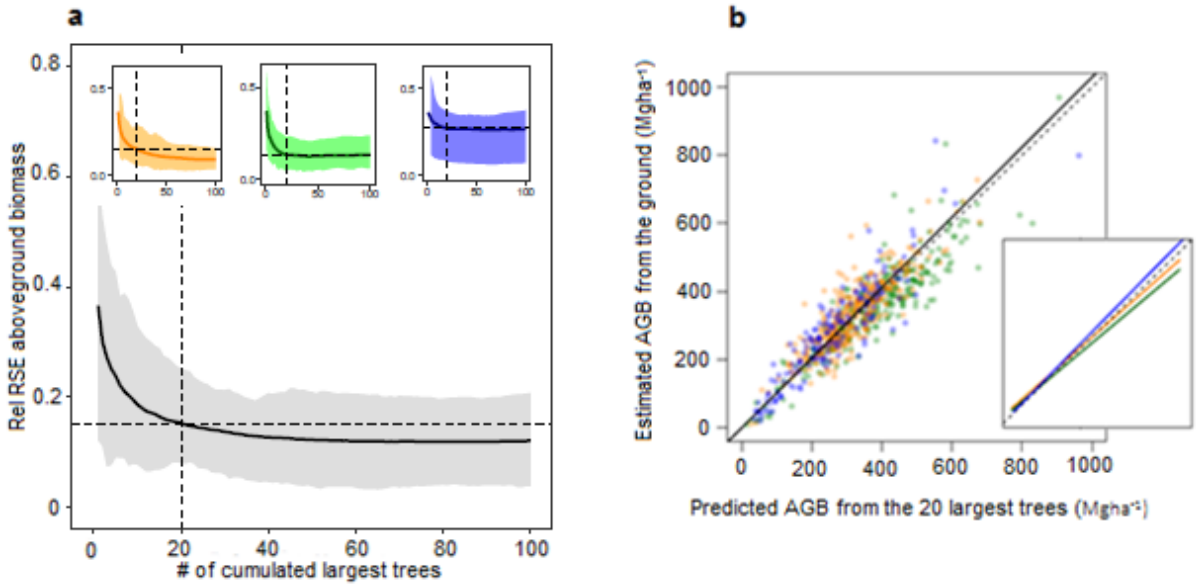

681

682 **Figure 4. Prediction of AGB from plot metrics of the 20 largest trees.** Results are shown
683 for the 867 plots, among the three continents colored orange, green and blue for America,
684 Africa and Asia respectively. The regression line of the model is shown as a continuous black
685 line while the dashed black line shows a 1:1 relationship. The figure shows an unbiased
686 prediction of AGB across the 867 plots, with slight but significant differences between the 3
687 continents.

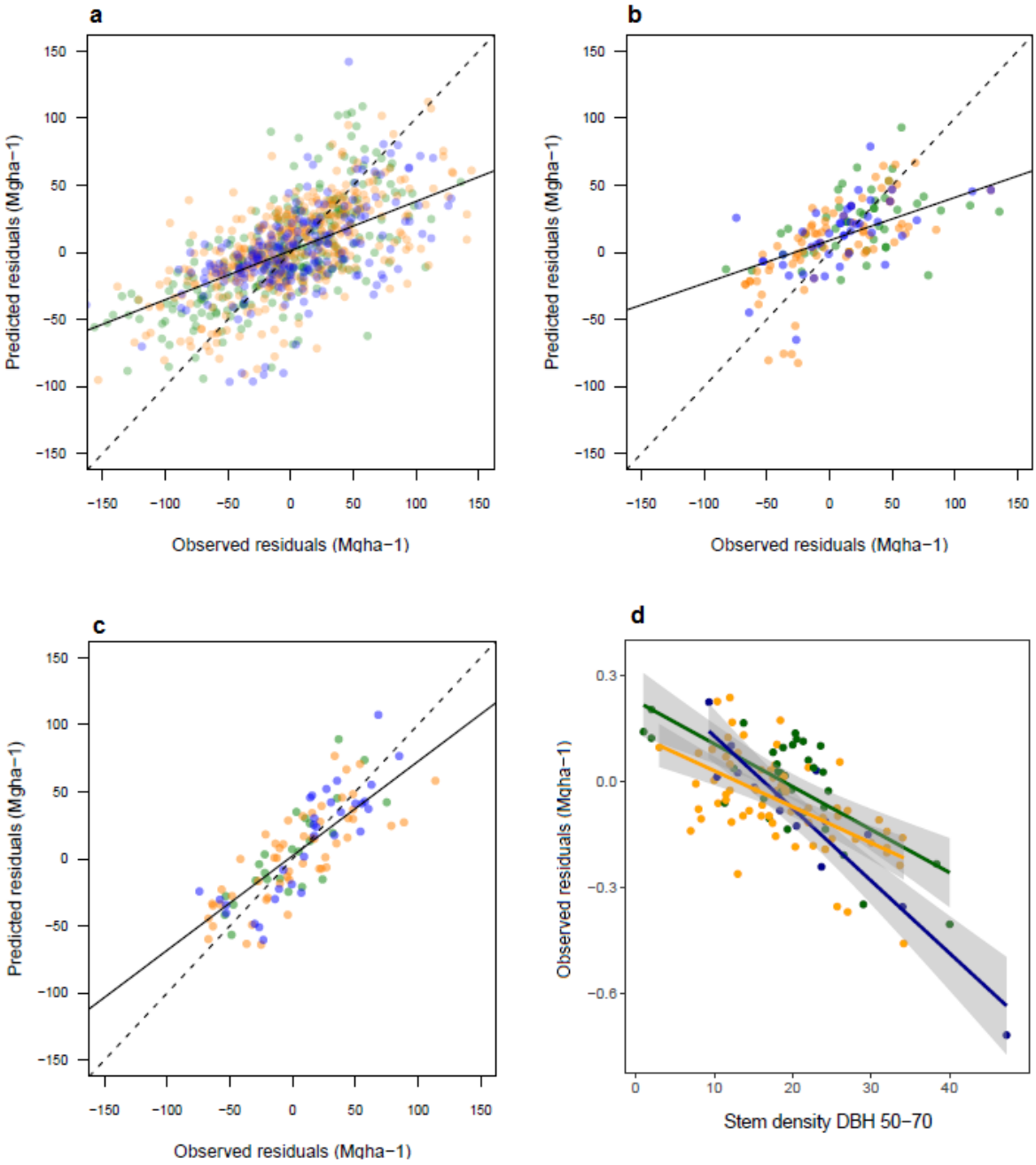

Figure 5. Predicted vs. observed residuals of aboveground biomass predicted from the 20 largest trees. Residuals are explored at three different levels: (a) plot, (b) site [without considering the diameter structure as an explanatory variable], (c) site [considering the diameter structure] and (d) along the stem density of medium size trees. America, Africa and Asia are colored in orange, green and blue respectively. The figures show a good prediction of residuals in (a) and (b), driven by stem density, and a less biased prediction in (c), driven by

695 the diameter structure. Variance of observed residuals are also well explained by the stem
696 density of medium size trees (d), which mainly drive the first axis of the PCA.

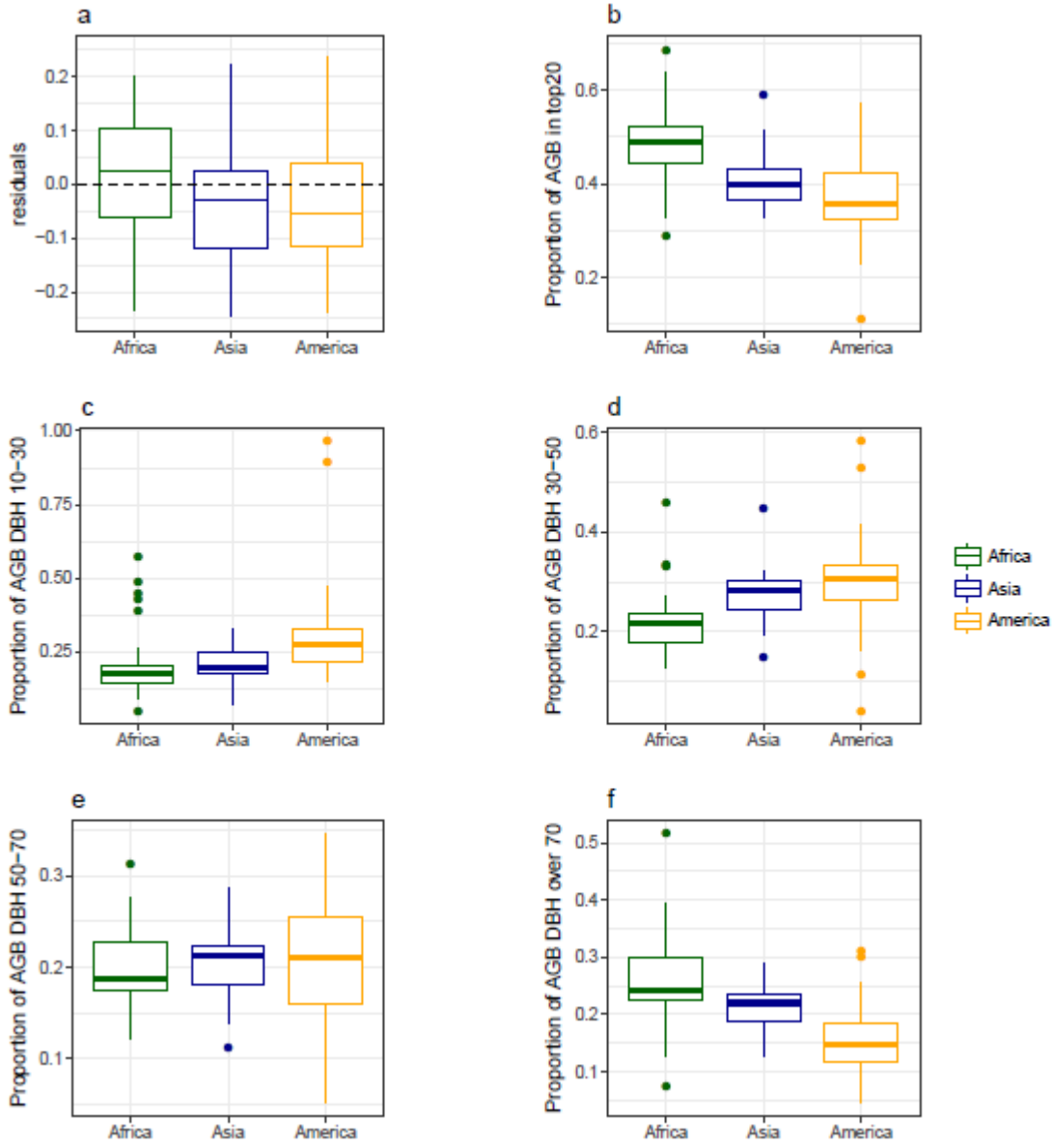

Figure 6. Comparison across continents of aboveground biomass prediction per site and their contribution to different share of the diameter structure. Africa, Asia and America, are colored in green, blue and orange, respectively. The distribution of the residuals of pan-tropical aboveground biomass prediction from the 20 largest trees (a) shows predictions are slightly overestimated in Africa (+3%), and slightly underestimated in Asia (-3%) and America (-5%). The proportion of aboveground biomass in the 20 largest trees (b) is highest in Africa (48%), followed by Asia (40%) and America (35%). The decomposition across four diameter classes (c-f, i.e. from 10 to 30, 30 to 50, 50 to 70 and beyond 70 cm) of their relative share of the total biomass shows that most of the biomass is found in the large trees in Africa, and in the small

707 to medium trees in America. Asia presenting a more balanced distribution of biomass across
708 the diameter structure.

709 **Tables**

710 **Table 1. Weight of each variable retained for the explanation of AGB residuals.** Weights
711 are calculated as a type II sum of squares, which measures the decreased residual sum of
712 squares due to an added variable once all the other variables have been introduced into the
713 model. Results are shown for the exploration of residuals at the plot and at the site level, with
714 and without consideration of the diameter structure. Weights are dominated by structural
715 variables, and in particular the stem density and the diameter structure. Height, wood density
716 and continent have also a non-negligible influence on residuals.

Level of residual	Parameter	Weight
Plot		
	Stem density*	79
	Continent*	18
	Lorey's height*	1
	Major soil types	1
	Temperature	1
	Wood density weighted by the basal area	0
	Rainfall	0
Site without diametric structure		
	Stem density*	54
	Continent*	28
	Wood density weighted by the basal area*	11
	Rainfall	3
	Major soil types	3
	Temperature	2
	Lorey's height	0
Site with diametric structure		
	PCA axis 1*	69
	Lorey's height*	23
	Rainfall*	3
	Major soil types	3
	Continent	1
	Temperature	1
	Wood density weighted by the basal area	0
	PCA axis 2	0

717

718 **References**

719 Asner, G.G.P., Mascaro, J., Muller-Landau, H.H.C., Vieilledent, G., Vaudry, R., Rasamoelina,
720 M., Hall, J.S. & van Breugel, M. (2012) A universal airborne LiDAR approach for tropical
721 forest carbon mapping. *Oecologia*, **168**, 1147–1160.

722 Asner, G.P., Martin, R.E., Knapp, D.E., Tupayachi, R., Anderson, C.B., Sinca, F., Vaughn,
723 N.R. & Llactayo, W. (2017) Airborne laser-guided imaging spectroscopy to map forest
724 trait diversity and guide conservation. *Science*, **355**.

725 Asner, G.P. & Mascaro, J. (2014) Mapping tropical forest carbon: Calibrating plot estimates
726 to a simple LiDAR metric. *Remote Sensing of Environment*, **140**, 614–624.

727 Baccini, A., Walker, W., Carvalho, L., Farina, M., Sulla-Menashe, D. & Houghton, R.A. (2017)
728 Tropical forests are a net carbon source based on aboveground measurements of gain
729 and loss. *Science (New York, N.Y.)*, **358**, 230–234.

730 Banin, L., Feldpausch, T.R., Phillips, O.L., Baker, T.R., Lloyd, J., Affum-Baffoe, K., Arets,
731 E.J.M.M., Berry, N.J., Bradford, M., Brienen, R.J.W., Davies, S., Drescher, M., Higuchi,
732 N., Hilbert, D.W., Hladik, a., Iida, Y., Salim, K.A., Kassim, a. R., King, D. a., Lopez-
733 Gonzalez, G., Metcalfe, D., Nilus, R., Peh, K.S.-H., Reitsma, J.M., Sonké, B.,
734 Taedoumg, H., Tan, S., White, L., Wöll, H. & Lewis, S.L. (2012) What controls tropical
735 forest architecture? Testing environmental, structural and floristic drivers. *Global*
736 *Ecology and Biogeography*, **21**, 1179–1190.

737 Bastin, J.-F., Barbier, N., Couteron, P., Adams, B., Shapiro, A., Bogaert, J., De Cannière, C.,
738 De Canniére, C. & De Cannière, C. (2014) Aboveground biomass mapping of African
739 forest mosaics using canopy texture analysis: toward a regional approach. *Ecological*
740 *Applications*, **24**, 1984–2001.

741 Bastin, J.F., Barbier, N., Réjou-Méchain, M., Fayolle, A., Gourlet-Fleury, S., Maniatis, D., De
742 Haulleville, T., Baya, F., Beeckman, H., Beina, D., Couteron, P., Chuyong, G., Dauby,
743 G., Doucet, J.L., Droissart, V., Dufrêne, M., Ewango, C., Gillet, J.F., Gonmadje, C.H.,
744 Hart, T., Kavali, T., Kenfack, D., Libalah, M., Malhi, Y., Makana, J.R., Pélissier, R.,
745 Ploton, P., Serckx, A., Sonké, B., Stevart, T., Thomas, D.W., De Cannière, C. &

746 Bogaert, J. (2015) Seeing Central African forests through their largest trees. *Scientific*
747 *Reports*, **5**, 13156.
748 Bastin, J.-F., Berrahmouni, N., Grainger, A., Maniatis, D., Mollicone, D., Moore, R., Patriarca,
749 C., Picard, N., Sparrow, B., Abraham, E.M., Aloui, K., Atesoglu, A., Attore, F., Bassüllü,
750 Ç., Bey, A., Garzuglia, M., García-Montero, L.G., Groot, N., Guerin, G., Laestadius, L.,
751 Lowe, A.J., Mamane, B., Marchi, G., Patterson, P., Rezende, M., Ricci, S., Salcedo, I.,
752 Diaz, A.S.-P., Stolle, F., Surappaeva, V. & Castro, R. (2017) The extent of forest in
753 dryland biomes. *Science*, **356**, 635–638.
754 Bennett, A.C., Mcdowell, N.G., Allen, C.D. & Anderson-Teixeira, K.J. (2015) Larger trees
755 suffer most during drought in forests worldwide. *Nature Plants*, **1**, 15139.
756 Blanchard, E., Birnbaum, P., Ibanez, T., Boutreux, T., Antin, C., Ploton, P., Vincent, G.,
757 Pouteau, R., Vandrot, H., Hequet, V., Barbier, N., Droissart, V., Sonké, B., Texier, N.,
758 Kamdem, N.G., Zebaze, D., Libalah, M. & Couteron, P. (2016) Contrasted allometries
759 between stem diameter, crown area, and tree height in five tropical biogeographic
760 areas. *Trees*, **30**, 1953–1968.
761 Carré, F., Hiederer, R., Blujdea, V. & Koeble, R. (2010) *Background guide for the calculation*
762 *of land carbon stocks in the biofuels sustainability scheme drawing on the 2006 IPCC*
763 *Guidelines for National Greenhouse Gas Inventories*, p128.
764 Chave, J., Coomes, D., Jansen, S., Lewis, S.L., Swenson, N.G. & Zanne, A.E. (2009)
765 Towards a worldwide wood economics spectrum. *Ecology letters*, **12**, 351–66.
766 Chave, J., Réjou-Méchain, M., Búrquez, A., Chidumayo, E., Colgan, M.S., Delitti, W.B.C.,
767 Duque, A., Eid, T., Fearnside, P.M., Goodman, R.C., Henry, M., Martínez-Yrízar, A.,
768 Mugasha, W.A., Muller-Landau, H.C., Mencuccini, M., Nelson, B.W., Ngomanda, A.,
769 Nogueira, E.M., Ortiz-Malavassi, E., Pélissier, R., Ploton, P., Ryan, C.M., Saldarriaga,
770 J.G. & Vieilledent, G. (2014) Improved allometric models to estimate the aboveground
771 biomass of tropical trees. *Global change biology*, **20**, 3177–3190.
772 Chave, J., Riera, B., Dubois, M.-A. & Riéra, B. (2001) Estimation of biomass in a neotropical
773 forest of French Guiana : spatial and temporal variability. *Journal of Tropical Ecology*,

774 **17**, 79–96.
775 Clark, D.B. & Clark, D.A. (1996) Abundance, growth and mortality of very large trees in
776 neotropical lowland rain forest. *Forest Ecology and Management*, **80**, 235–244.
777 Clark, D.B. & Clark, D.A. (2000) Landscape-scale variation in forest structure and biomass in
778 a tropical rain forest. *Forest Ecology and Management*, **137**, 185–198.
779 Clark, D.B. & Kellner, J.R. (2012) Tropical forest biomass estimation and the fallacy of
780 misplaced concreteness. *Journal of Vegetation Science*, **23**, 1191–1196.
781 Coomes, D.A., Dalponte, M., Jucker, T., Asner, G.P., Banin, L.F., Burslem, D.F.R.P., Lewis,
782 S.L., Nilus, R., Phillips, O.L., Phua, M.-H. & Qie, L. (2017) Area-based vs tree-centric
783 approaches to mapping forest carbon in Southeast Asian forests from airborne laser
784 scanning data. *Remote Sensing of Environment*, **194**, 77–88.
785 Coomes, D.A., Šafka, D., Shepherd, J., Dalponte, M. & Holdaway, R. (2018) Airborne laser
786 scanning of natural forests in New Zealand reveals the influences of wind on forest
787 carbon. *Forest Ecosystems 2017 5:1*, **5**, 10.
788 D'Oliveira, M.V.N., Reutebuch, S.E., McGaughey, R.J. & Andersen, H.-E. (2012) Estimating
789 forest biomass and identifying low-intensity logging areas using airborne scanning lidar
790 in Antimary State Forest, Acre State, Western Brazilian Amazon. *Remote Sensing of*
791 *Environment*, **124**, 479–491.
792 Dubayah, R., Goetz, S.J., Blair, J.B., Fatoyinbo, T.E., Hansen, M., Healey, S.P., Hofton,
793 M.A., Hurtt, G.C., Kellner, J., Luthcke, S.B. & Swatantran, A. (2014) The Global
794 Ecosystem Dynamics Investigation. *American Geophysical Union, Fall Meeting 2014,*
795 *abstract id. U14A-07*.
796 Enquist, B.J., West, G.B. & Brown, J.H. (2009) Extensions and evaluations of a general
797 quantitative theory of forest structure and dynamics. *Proceedings of the National*
798 *Academy of Sciences*, **106**, 7046–7051.
799 Farrior, C.E., Bohlman, S.A., Hubbell, S. & Pacala, S.W. (2016) Dominance of the
800 suppressed: Power-law size structure in tropical forests. *Science*, **351**.
801 Fayolle, A., Loubota Panzou, G.J., Drouet, T., Swaine, M.D., Bauwens, S., Vleminckx, J.,

802 Biwole, A., Lejeune, P. & Doucet, J.-L. (2016) Taller trees, denser stands and greater
803 biomass in semi-deciduous than in evergreen lowland central African forests. *Forest*
804 *Ecology and Management*, **374**, 42–50.
805 Feldpausch, T.R., Banin, L., Phillips, O.L., Baker, T.R., Lewis, S.L., Quesada, C. a., Affum-
806 Baffoe, K., Arets, E.J.M.M., Berry, N.J., Bird, M., Brondizio, E.S., de Camargo, P.,
807 Chave, J., Djagbletey, G., Domingues, T.F., Drescher, M., Fearnside, P.M., França,
808 M.B., Fyllas, N.M., Lopez-Gonzalez, G., Hladik, a., Higuchi, N., Hunter, M.O., Iida, Y.,
809 Salim, K. a., Kassim, a. R., Keller, M., Kemp, J., King, D. a., Lovett, J.C., Marimon,
810 B.S., Marimon-Junior, B.H., Lenza, E., Marshall, a. R., Metcalfe, D.J., Mitchard, E.T. a.,
811 Moran, E.F., Nelson, B.W., Nilus, R., Nogueira, E.M., Palace, M., Patiño, S., Peh, K.S.-
812 H., Raventos, M.T., Reitsma, J.M., Saiz, G., Schrodt, F., Sonké, B., Taedoumg, H.E.,
813 Tan, S., White, L., Wöll, H. & Lloyd, J. (2011) Height-diameter allometry of tropical forest
814 trees. *Biogeosciences*, **8**, 1081–1106.
815 Feldpausch, T.R., Lloyd, J., Lewis, S.L., Brienen, R.J.W., Gloor, M., Monteagudo Mendoza,
816 A., Lopez-Gonzalez, G., Banin, L., Abu Salim, K., Affum-Baffoe, K., Alexiades, M.,
817 Almeida, S., Amaral, I., Andrade, A., Aragão, L.E.O.C., Araujo Murakami, A., Arets,
818 E.J.M.M., Arroyo, L., Aymard C., G.A., Baker, T.R., Bánki, O.S., Berry, N.J., Cardozo,
819 N., Chave, J., Comiskey, J.A., Alvarez, E., de Oliveira, A., Di Fiore, A., Djagbletey, G.,
820 Domingues, T.F., Erwin, T.L., Fearnside, P.M., França, M.B., Freitas, M.A., Higuchi, N.,
821 E. Honorio C., Iida, Y., Jiménez, E., Kassim, A.R., Killeen, T.J., Laurance, W.F., Lovett,
822 J.C., Malhi, Y., Marimon, B.S., Marimon-Junior, B.H., Lenza, E., Marshall, A.R.,
823 Mendoza, C., Metcalfe, D.J., Mitchard, E.T.A., Neill, D.A., Nelson, B.W., Nilus, R.,
824 Nogueira, E.M., Parada, A., Peh, K.S.-H., Pena Cruz, A., Peñuela, M.C., Pitman,
825 N.C.A., Prieto, A., Quesada, C.A., Ramírez, F., Ramírez-Angulo, H., Reitsma, J.M.,
826 Rudas, A., Saiz, G., Salomão, R.P., Schwarz, M., Silva, N., Silva-Espejo, J.E., Silveira,
827 M., Sonké, B., Stropp, J., Taedoumg, H.E., Tan, S., ter Steege, H., Terborgh, J.,
828 Torello-Raventos, M., van der Heijden, G.M.F., Vásquez, R., Vilanova, E., Vos, V.A.,
829 White, L., Willcock, S., Woell, H. & Phillips, O.L. (2012) Tree height integrated into

pantropical forest biomass estimates. *Biogeosciences*, **9**, 3381–3403.

Ferraz, A., Saatchi, S., Mallet, C. & Meyer, V. (2016) Lidar detection of individual tree size in tropical forests. *Remote Sensing of Environment*, **183**, 318–333.

Gibbs, H.K., Brown, S., Niles, J.O. & Foley, J. a (2007) Monitoring and estimating tropical forest carbon stocks: making REDD a reality. *Environmental Research Letters*, **2**, 1–13.

Harms, K.E., Wright, S.J., Calderón, O., Hernández, a & Herre, E. a (2000) Pervasive density-dependent recruitment enhances seedling diversity in a tropical forest. *Nature*, **404**, 493–5.

Ho Tong Minh, D., Le Toan, T., Rocca, F., Tebaldini, S., Villard, L., Réjou-Méchain, M., Phillips, O.L., Feldpausch, T.R., Dubois-Fernandez, P., Scipal, K. & Chave, J. (2016) SAR tomography for the retrieval of forest biomass and height: Cross-validation at two tropical forest sites in French Guiana. *Remote Sensing of Environment*, **175**, 138–147.

IPCC (2006) *2006 IPCC Guidelines for National Greenhouse Gas Inventories, Prepared by the National Greenhouse Gas Inventories Programme*, IGES. (ed. by H.S. Eggleston), L. Buendia), K. Miwa), T. Ngara), and K. Tanabe) Japan, Japan.

Jucker, T., Bongalov, B., Burslem, D.F.R.P., Nilus, R., Dalponte, M., Lewis, S.L., Phillips, O.L., Qie, L. & Coomes, D.A. (2018) Topography shapes the structure, composition and function of tropical forest landscapes. *Ecology Letters*.

Jucker, T., Caspersen, J., Chave, J., Antin, C., Barbier, N., Bongers, F., Dalponte, M., van Ewijk, K.Y., Forrester, D.I., Haeni, M., Higgins, S.I., Holdaway, R.J., Iida, Y., Lorimer, C., Marshall, P.L., Momo, S., Moncrieff, G.R., Ploton, P., Poorter, L., Rahman, K.A., Schlund, M., Sonké, B., Sterck, F.J., Trugman, A.T., Usoltsev, V.A., Vanderwel, M.C., Waldner, P., Wedeux, B.M.M., Wirth, C., Wöll, H., Woods, M., Xiang, W., Zimmermann, N.E. & Coomes, D.A. (2017) Allometric equations for integrating remote sensing imagery into forest monitoring programmes. *Global Change Biology*, **23**, 177–190.

Kearsley, E., de Haulleville, T., Hufkens, K., Kidimbu, A., Toirambe, B., Baert, G., Huygens, D., Kebede, Y., Defourny, P., Bogaert, J., Beeckman, H., Steppe, K., Boeckx, P. & Verbeeck, H. (2013) Conventional tree height-diameter relationships significantly

858 overestimate aboveground carbon stocks in the Congo Basin. *Nature communications*.
859 Kellner, J.R., Clark, D.B. & Hubbell, S.P. (2009) Pervasive canopy dynamics produce short-
860 term stability in a tropical rain forest landscape. *Ecology Letters*, **12**, 155–164.
861 Kellner, J.R. & Hubbell, S.P. (2017) Adult mortality in a low-density tree population using
862 high-resolution remote sensing. *Ecology*, **98**, 1700–1709.
863 Langsrud, Ø. (2003) ANOVA for unbalanced data: Use Type II instead of Type III sums of
864 squares. *Statistics and Computing*, **13**, 163–167.
865 Laurance, W.F., Delamônica, P., Laurance, S.G., Vasconcelos, H.L. & Lovejoy, T.E. (2000)
866 Conservation: Rainforest fragmentation kills big trees. *Nature*, **404**, 836–836.
867 Lewis, S.L., Sonké, B., Sunderland, T., Begne, S.K., Lopez-Gonzalez, G., van der Heijden,
868 G.M.F., Phillips, O.L., Affum-Baffoe, K., Baker, T.R., Banin, L., Bastin, J.-F., Beeckman,
869 H., Boeckx, P., Bogaert, J., De Cannière, C., Chezeaux, E., Clark, C.J., Collins, M.,
870 Djagbletey, G., Djuikouo, M.N.K., Droissart, V., Doucet, J.-L., Ewango, C.E.N., Fauset,
871 S., Feldpausch, T.R., Foli, E.G., Gillet, J.-F., Hamilton, A.C., Harris, D.J., Hart, T.B., de
872 Haulleville, T., Hladik, A., Hufkens, K., Huygens, D., Jeanmart, P., Jeffery, K.J.,
873 Kearsley, E., Leal, M.E., Lloyd, J., Lovett, J.C., Makana, J.-R., Malhi, Y., Marshall, A.R.,
874 Ojo, L., Peh, K.S.-H., Pickavance, G., Poulsen, J.R., Reitsma, J.M., Sheil, D., Simo, M.,
875 Steppe, K., Taedoumg, H.E., Talbot, J., Taplin, J.R.D., Taylor, D., Thomas, S.C.,
876 Toirambe, B., Verbeeck, H., Vleminckx, J., White, L.J.T., Willcock, S., Woell, H. &
877 Zemagho, L. (2013) Above-ground biomass and structure of 260 African tropical forests.
878 *Philosophical Transactions of the Royal Society B: Biological Sciences*, **368**, 20120295.
879 Lindenmayer, D.B., Laurance, W.F. & Franklin, J.F. (2012) Global decline in large old trees.
880 *Science*, **338**, 1305–1306.
881 Lutz, J.A., Furniss, T.J., Johnson, D.J., Davies, S.J., Allen, D., Alonso, A., Anderson-
882 Teixeira, K.J., Andrade, A., Baltzer, J., Becker, K.M.L., Blomdahl, E.M., Bourg, N.A.,
883 Bunyavejchewin, S., Burslem, D.F.R.P., Cansler, C.A., Cao, K., Cao, M., Cárdenas, D.,
884 Chang, L.-W., Chao, K.-J., Chao, W.-C., Chiang, J.-M., Chu, C., Chuyong, G.B., Clay,
885 K., Condit, R., Cordell, S., Dattaraja, H.S., Duque, A., Ewango, C.E.N., Fischer, G.A.,

886 Fletcher, C., Freund, J.A., Giardina, C., Germain, S.J., Gilbert, G.S., Hao, Z., Hart, T.,
887 Hau, B.C.H., He, F., Hector, A., Howe, R.W., Hsieh, C.-F., Hu, Y.-H., Hubbell, S.P.,
888 Inman-Narahari, F.M., Itoh, A., Janík, D., Kassim, A.R., Kenfack, D., Korte, L., Král, K.,
889 Larson, A.J., Li, Y., Lin, Y., Liu, S., Lum, S., Ma, K., Makana, J.-R., Malhi, Y., McMahon,
890 S.M., McShea, W.J., Memiaghe, H.R., Mi, X., Morecroft, M., Musili, P.M., Myers, J.A.,
891 Novotny, V., de Oliveira, A., Ong, P., Orwig, D.A., Ostertag, R., Parker, G.G., Patankar,
892 R., Phillips, R.P., Reynolds, G., Sack, L., Song, G.-Z.M., Su, S.-H., Sukumar, R., Sun,
893 I.-F., Suresh, H.S., Swanson, M.E., Tan, S., Thomas, D.W., Thompson, J., Uriarte, M.,
894 Valencia, R., Vicentini, A., Vrška, T., Wang, X., Weiblen, G.D., Wolf, A., Wu, S.-H., Xu,
895 H., Yamakura, T., Yap, S. & Zimmerman, J.K. (2018) Global importance of large-
896 diameter trees. *Global Ecology and Biogeography*. **00**, 1–16.
897 Malhi, Y., Wood, D., Baker, T.R., Wright, J., Phillips, O.L., Cochrane, T., Meir, P., Chave, J.,
898 Almeida, S., Arroyo, L., Higuchi, N., Killeen, T.J., Laurance, S.G., Laurance, W.F.,
899 Lewis, S.L., Monteagudo, A., Neill, D. a., Vargas, P.N., Pitman, N.C. a., Quesada, C.A.,
900 Salomao, R., Silva, J.N.M., Lezama, A.T., Terborgh, J., Martinez, R.V. & Vinceti, B.
901 (2006) The regional variation of aboveground live biomass in old-growth Amazonian
902 forests. *Global Change Biology*, **12**, 1107–1138.
903 Maniatis, D. & Mollicone, D. (2010) Options for sampling and stratification for national forest
904 inventories to implement REDD+ under the UNFCCC. *Carbon balance and*
905 *management*, **5**, 9.
906 Mascaro, J., Detto, M., Asner, G.P. & Muller-Landau, H.C. (2011) Evaluating uncertainty in
907 mapping forest carbon with airborne LiDAR. *Remote Sensing of Environment*, **115**,
908 3770–3774.
909 Meakem, V., Tepley, A.J., Gonzalez-Akre, E.B., Herrmann, V., Muller-Landau, H.C., Wright,
910 S.J., Hubbell, S.P., Condit, R. & Anderson-Teixeira, K.J. (2017) Role of tree size in
911 moist tropical forest carbon cycling and water deficit responses. *New Phytologist*.
912 Molto, Q., Hérault, B., Boreux, J.-J., Daullet, M., Rousteau, A. & Rossi, V. (2014) Predicting
913 tree heights for biomass estimates in tropical forests – a test from French Guiana.

914 *Biogeosciences*, **11**, 3121–3130.
915 Nepstad, D.C., Tohver, I.M., Ray, D., Moutinho, P. & Cardinot, G. (2007) Mortality of large
916 trees and lianas following experimental drought in an Amazon forest. *Ecology*, **88**,
917 2259–69.
918 New, M., Hulme, M., Jones, P., New, M., Hulme, M. & Jones, P. (1999) Representing
919 Twentieth-Century Space–Time Climate Variability. Part I: Development of a 1961–90
920 Mean Monthly Terrestrial Climatology. *Journal of Climate*, **12**, 829–856.
921 New, M., Lister, D., Hulme, M. & Makin, I. (2002) A high-resolution data set of surface
922 climate over global land areas. *Climate Research*, **21**, 1–25.
923 Ploton, P., Barbier, N., Couteron, P., Antin, C.M., Ayyappan, N., Balachandran, N., Barathan,
924 N., Bastin, J.-F., Chuyong, G., Dauby, G., Droissart, V., Gastellu-Etchegorry, J.-P.,
925 Kamdem, N.G., Kenfack, D., Libalah, M., Mofack, G., Momo, S.T., Pargal, S., Petronelli,
926 P., Proisy, C., Réjou-Méchain, M., Sonké, B., Texier, N., Thomas, D., Verley, P.,
927 Zebaze Dongmo, D., Berger, U. & Pélissier, R. (2017) Toward a general tropical forest
928 biomass prediction model from very high resolution optical satellite images. *Remote*
929 *Sensing of Environment*, **200**, 140–153.
930 Ploton, P., Barbier, N., Takoudjou Momo, S., Réjou-Méchain, M., Boyemba Bosela, F.,
931 Chuyong, G., Dauby, G., Droissart, V., Fayolle, A., Goodman, R.C., Henry, M.,
932 Kamdem, N.G., Mukirania, J.K., Kenfack, D., Libalah, M., Ngomanda, A., Rossi, V.,
933 Sonké, B., Texier, N., Thomas, D., Zebaze, D., Couteron, P., Berger, U. & Pélissier, R.
934 (2016) Closing a gap in tropical forest biomass estimation: taking crown mass variation
935 into account in pantropical allometries. *Biogeosciences*, **13**, 1571–1585.
936 Ploton, P., Pélissier, R. & Proisy, C. (2012) Assessing aboveground tropical forest biomass
937 using Google Earth canopy images. *Ecological Applications*, **22**, 993–1003.
938 Poorter, L., van der Sande, M.T., Thompson, J., Arets, E.J.M.M., Alarcón, A., Álvarez-
939 Sánchez, J., Ascarrunz, N., Balvanera, P., Barajas-Guzmán, G., Boit, A., Bongers, F.,
940 Carvalho, F.A., Casanoves, F., Cornejo-Tenorio, G., Costa, F.R.C., de Castilho, C. V.,
941 Duivenvoorden, J.F., Dutrieux, L.P., Enquist, B.J., Fernández-Méndez, F., Finegan, B.,

942 Gormley, L.H.L., Healey, J.R., Hoosbeek, M.R., Ibarra-Manríquez, G., Junqueira, A.B.,
943 Levis, C., Licona, J.C., Lisboa, L.S., Magnusson, W.E., Martínez-Ramos, M., Martínez-
944 Yrizar, A., Martorano, L.G., Maskell, L.C., Mazzei, L., Meave, J.A., Mora, F., Muñoz, R.,
945 Nytch, C., Pansonato, M.P., Parr, T.W., Paz, H., Pérez-García, E.A., Rentería, L.Y.,
946 Rodríguez-Velazquez, J., Rozendaal, D.M.A., Ruschel, A.R., Sakschewski, B., Salgado-
947 Negret, B., Schietti, J., Simões, M., Sinclair, F.L., Souza, P.F., Souza, F.C., Stropp, J.,
948 ter Steege, H., Swenson, N.G., Thonicke, K., Toledo, M., Uriarte, M., van der Hout, P.,
949 Walker, P., Zamora, N. & Peña-Claros, M. (2015) Diversity enhances carbon storage in
950 tropical forests. *Global Ecology and Biogeography*, **24**, 1314–1328.
951 Proisy, C., Couteron, P. & Fromard, F. (2007) Predicting and mapping mangrove biomass
952 from canopy grain analysis using Fourier-based textural ordination of IKONOS images.
953 *Remote Sensing of Environment*, **109**, 379–392.
954 Réjou-Méchain, M., Tanguy, A., Piponiot, C., Chave, J. & Hérault, B. (2017) biomass : an r
955 package for estimating above-ground biomass and its uncertainty in tropical forests.
956 *Methods in Ecology and Evolution*, **8**, 1163–1167.
957 Remm, J. & Lõhmus, A. (2011) Tree cavities in forests – The broad distribution pattern of a
958 keystone structure for biodiversity. *Forest Ecology and Management*, **262**, 579–585.
959 Romijn, E., Herold, M., Kooistra, L., Murdiyarso, D. & Verchot, L. (2012) Assessing
960 capacities of non-Annex I countries for national forest monitoring in the context of
961 REDD+. *Environmental Science & Policy*, **19**–**20**, 33–48.
962 Rutishauser, E., Hérault, B., Baraloto, C., Blanc, L., Descroix, L., Sotta, E.D., Ferreira, J.,
963 Kanashiro, M., Mazzei, L., d'Oliveira, M.V.N., de Oliveira, L.C., Peña-Claros, M., Putz,
964 F.E., Ruschel, A.R., Rodney, K., Roopsind, A., Shenkin, A., da Silva, K.E., de Souza,
965 C.R., Toledo, M., Vidal, E., West, T.A.P., Wortel, V. & Sist, P. (2015) Rapid tree carbon
966 stock recovery in managed Amazonian forests. *Current biology : CB*, **25**, R787-8.
967 Rutishauser, E., Wagner, F., Herault, B., Nicolini, E.-A. & Blanc, L. (2010) Contrasting above-
968 ground biomass balance in a Neotropical rain forest. *Journal of Vegetation Science*,
969 672–682.

970 Saatchi, S.S., Houghton, R. a., Dos Santos Alvalá, R.C., Soares, J. V. & Yu, Y. (2007)
971 Distribution of aboveground live biomass in the Amazon basin. *Global Change Biology*,
972 **13**, 816–837.
973 Sist, P., Mazzei, L., Blanc, L. & Rutishauser, E. (2014) Large trees as key elements of
974 carbon storage and dynamics after selective logging in the Eastern Amazon. *Forest*
975 *Ecology and Management*, **318**, 103–109.
976 Slik, J.W.F., Aiba, S.-I., Brearley, F.Q., Cannon, C.H., Forshed, O., Kitayama, K., Nagamasu,
977 H., Nilus, R., Payne, J., Paoli, G., Poulsen, A.D., Raes, N., Sheil, D., Sidiyasa, K.,
978 Suzuki, E. & Van Valkenburg, J.L.C.H. (2010) Environmental correlates of tree biomass,
979 basal area, wood specific gravity and stem density gradients in Borneo's tropical forests.
980 *Global Ecology and Biogeography*, **19**, 50–60.
981 Slik, J.W.F., Alvarez-loayza, P., Alves, L.F., Ashton, P., Balvanera, P., Bastian, M.L.,
982 Bellingham, P.J., Berg, E. Van Den, Bernacci, L., Conceição, P., Blanc, L., Böhning-
983 gaese, K., Boeckx, P., Boyle, B., Bradford, M., Brearley, F.Q., Hockemba, B.,
984 Bunyavejchewin, S., Matos, C.L., Castillo-santiago, M., Eduardo, L.M., Chai, S., Chen,
985 Y., Colwell, R.K., Robin, C.L., Clark, C., Clark, D.B., Deborah, A., Culmsee, H., Damas,
986 K., Dattaraja, H.S., Dauby, G., Davidar, P., Dewalt, S.J., Doucet, J., Duque, A., Durigan,
987 G., Eichhorn, K.A.O., Pedro, V., Eler, E., Ewango, C., Farwig, N., Feeley, K.J., Ferreira,
988 L., Field, R., Ary, T., Filho, D.O., Fletcher, C., Forshed, O., Fredriksson, G., Gillespie, T.,
989 Amarnath, G., Griffith, D.M., Grogan, J., Gunatilleke, N., Harris, D., Harrison, R., Hector,
990 A., Homeier, J., Imai, N., Itoh, A., Jansen, P.A., Joly, C.A., Jong, B.H.J. De,
991 Kartawinata, K., Kearsley, E., Kelly, D.L., Kenfack, D., Kitayama, K., Kooyman, R.,
992 Larney, E., Laurance, S., Laurance, W.F., Michael, J., Leao, I., Letcher, S.G., Lindsell,
993 J., Lu, X., Mansor, A., Marjokorpi, A., Martin, E.H., Meilby, H., Melo, F.P.L., Metcalfe,
994 D.J., Vincent, P., Metzger, J.P., Millet, J., Mohandass, D., Juan, C., Nagamasu, H.,
995 Nilus, R., Ochoa-gaona, S., Paudel, E., Permana, A., Maria, T.F., Rovero, F., Rozak,
996 A.H., Santos, B.A., Santos, F., Sarker, S.K., Satdichanh, M., Schmitt, C.B., Schöngart,
997 J., Tabarelli, M., Tang, J., Targhetta, N., Theilade, I., Thomas, D.W., Tchouto, P.,

998 Hurtado, J., Valkenburg, J.L.C.H. Van, Do, T. Van, Verbeeck, H., Adekunle, V., Vieira,
999 S.A., Alvarez-loayza, P., Alves, L.F., Berg, E. Van Den & Bernacci, L. (2015) An
1000 estimate of the number of tropical tree species. *Proceedings of the National Academy of*
1001 *Sciences*, **112**, E4628–E4629.
1002 Slik, J.W.F., Franklin, J., Arroyo-Rodríguez, V., Field, R., Aguilar, S., Aguirre, N., Ahumada,
1003 J., Aiba, S.-I., Alves, L.F., K, A., Avella, A., Mora, F., Aymard C., G.A., Báez, S.,
1004 Balvanera, P., Bastian, M.L., Bastin, J.-F., Bellingham, P.J., van den Berg, E., da
1005 Conceição Bispo, P., Boeckx, P., Boehning-Gaese, K., Bongers, F., Boyle, B.,
1006 Brambach, F., Brearley, F.Q., Brown, S., Chai, S.-L., Chazdon, R.L., Chen, S., Chhang,
1007 P., Chuyong, G., Ewango, C., Coronado, I.M., Cristóbal-Azkarate, J., Culmsee, H.,
1008 Damas, K., Dattaraja, H.S., Davidar, P., DeWalt, S.J., Din, H., Drake, D.R., Duque, A.,
1009 Durigan, G., Eichhorn, K., Eler, E.S., Enoki, T., Ensslin, A., Fandohan, A.B., Farwig, N.,
1010 Feeley, K.J., Fischer, M., Forshed, O., Garcia, Q.S., Garkoti, S.C., Gillespie, T.W.,
1011 Gillet, J.-F., Gonmadje, C., Granzow-de la Cerda, I., Griffith, D.M., Grogan, J., Hakeem,
1012 K.R., Harris, D.J., Harrison, R.D., Hector, A., Hemp, A., Homeier, J., Hussain, M.S.,
1013 Ibarra-Manríquez, G., Hanum, I.F., Imai, N., Jansen, P.A., Joly, C.A., Joseph, S.,
1014 Kartawinata, K., Kearsley, E., Kelly, D.L., Kessler, M., Killeen, T.J., Kooyman, R.M.,
1015 Laumonier, Y., Laurance, S.G., Laurance, W.F., Lawes, M.J., Letcher, S.G., Lindsell, J.,
1016 Lovett, J., Lozada, J., Lu, X., Lykke, A.M., Mahmud, K. Bin, Mahayani, N.P.D., Mansor,
1017 A., Marshall, A.R., Martin, E.H., Calderado Leal Matos, D., Meave, J.A., Melo, F.P.L.,
1018 Mendoza, Z.H.A., Metali, F., Medjibe, V.P., Metzger, J.P., Metzker, T., Mohandass, D.,
1019 Munguía-Rosas, M.A., Muñoz, R., Nurtjahy, E., de Oliveira, E.L., Onrizal, Parolin, P.,
1020 Parren, M., Parthasarathy, N., Paudel, E., Perez, R., Pérez-García, E.A., Pommer, U.,
1021 Poorter, L., Qi, L., Piedade, M.T.F., Pinto, J.R.R., Poulsen, A.D., Poulsen, J.R., Powers,
1022 J.S., Prasad, R.C., Puyravaud, J.-P., Rangel, O., Reitsma, J., Rocha, D.S.B., Rolim, S.,
1023 Rovero, F., Rozak, A., Ruokolainen, K., Rutishauser, E., Rutten, G., Mohd. Said, M.N.,
1024 Saiter, F.Z., Saner, P., Santos, B., dos Santos, J.R., Sarker, S.K., Schmitt, C.B.,
1025 Schoengart, J., Schulze, M., Sheil, D., Sist, P., Souza, A.F., Spironello, W.R., Sposito,

1026 T., Steinmetz, R., Stevart, T., Suganuma, M.S., Sukri, R., Sultana, A., Sukumar, R.,
1027 Sunderland, T., Supriyadi, Suresh, H.S., Suzuki, E., Tabarelli, M., Tang, J., Tanner,
1028 E.V.J., Targhetta, N., Theilade, I., Thomas, D., Timberlake, J., de Morisson Valeriano,
1029 M., van Valkenburg, J., Van Do, T., Van Sam, H., Vandermeer, J.H., Verbeeck, H.,
1030 Vetaas, O.R., Adekunle, V., Vieira, S.A., Webb, C.O., Webb, E.L., Whitfeld, T., Wich, S.,
1031 Williams, J., Wiser, S., Wittmann, F., Yang, X., Adou Yao, C.Y., Yap, S.L., Zahawi, R.A.,
1032 Zakaria, R. & Zang, R. (2018) Phylogenetic classification of the world's tropical forests.
1033 *Proceedings of the National Academy of Sciences*, **115**, 1837–1842.
1034 Slik, J.W.F., Paoli, G., McGuire, K., Amaral, I., Barroso, J., Bastian, M., Blanc, L., Bongers,
1035 F., Boundja, P., Clark, C., Collins, M., Dauby, G., Ding, Y., Doucet, J.-L., Eler, E.,
1036 Ferreira, L., Forshed, O., Fredriksson, G., Gillet, J.-F., Harris, D., Leal, M., Laumonier,
1037 Y., Malhi, Y., Mansor, A., Martin, E., Miyamoto, K., Araujo-Murakami, A., Nagamasu, H.,
1038 Nilus, R., Nurtjahya, E., Oliveira, Á., Onrizal, O., Parada-Gutierrez, A., Permana, A.,
1039 Poorter, L., Poulsen, J., Ramirez-Angulo, H., Reitsma, J., Rovero, F., Rozak, A., Sheil,
1040 D., Silva-Espejo, J., Silveira, M., Spironelo, W., ter Steege, H., Stevart, T., Navarro-
1041 Aguilar, G.E., Sunderland, T., Suzuki, E., Tang, J., Theilade, I., van der Heijden, G., van
1042 Valkenburg, J., Van Do, T., Vilanova, E., Vos, V., Wich, S., Wöll, H., Yoneda, T., Zang,
1043 R., Zhang, M.-G. & Zweifel, N. (2013) Large trees drive forest aboveground biomass
1044 variation in moist lowland forests across the tropics. *Global Ecology and Biogeography*,
1045 **22**, 1261–1271.
1046 Stark, S.C., Enquist, B.J., Saleska, S.R., Leitold, V., Schietti, J., Longo, M., Alves, L.F.,
1047 Camargo, P.B. & Oliveira, R.C. (2015) Linking canopy leaf area and light environments
1048 with tree size distributions to explain Amazon forest demography. *Ecology Letters*, **18**,
1049 636–645.
1050 Stark, S.C., Leitold, V., Wu, J.L., Hunter, M.O., de Castilho, C. V., Costa, F.R.C., Mcmahon,
1051 S.M., Parker, G.G., Shimabukuro, M.T., Lefsky, M.A., Keller, M., Alves, L.F., Schietti, J.,
1052 Shimabukuro, Y.E., Brand??o, D.O., Woodcock, T.K., Higuchi, N., de Camargo, P.B.,
1053 de Oliveira, R.C. & Saleska, S.R. (2012) Amazon forest carbon dynamics predicted by

profiles of canopy leaf area and light environment. *Ecology Letters*, **15**, 1406–1414.

Stegen, J.C., Swenson, N.G., Enquist, B.J., White, E.P., Phillips, O.L., Jørgensen, P.M., Weiser, M.D., Monteagudo Mendoza, A. & Núñez Vargas, P. (2011) Variation in above-ground forest biomass across broad climatic gradients. *Global Ecology and Biogeography*, **20**, 744–754.

Sullivan, M.J.P., Lewis, S.L., Hubau, W., Qie, L., Baker, T.R., Banin, L.F., Chave, J., Cuni-Sanchez, A., Feldpausch, T.R., Lopez-Gonzalez, G., Arets, E., Ashton, P., Bastin, J.-F., Berry, N.J., Bogaert, J., Boot, R., Brearley, F.Q., Brienen, R., Burslem, D.F.R.P., de Canniere, C., Chudomelová, M., Dančák, M., Ewango, C., Hédl, R., Lloyd, J., Makana, J.-R., Malhi, Y., Marimon, B.S., Junior, B.H.M., Metali, F., Moore, S., Nagy, L., Vargas, P.N., Pendry, C.A., Ramírez-Angulo, H., Reitsma, J., Rutishauser, E., Salim, K.A., Sonké, B., Sukri, R.S., Sunderland, T., Svátek, M., Umunay, P.M., Martinez, R.V., Vernimmen, R.R.E., Torre, E.V., Vleminckx, J., Vos, V. & Phillips, O.L. (2018) Field methods for sampling tree height for tropical forest biomass estimation. *Methods in Ecology and Evolution*, **9**, 1179–1189.

Sullivan, M.J.P., Talbot, J., Lewis, S.L., Phillips, O.L., Qie, L., Begne, S.K., Chave, J., Cuni-Sanchez, A., Hubau, W., Lopez-Gonzalez, G., Miles, L., Monteagudo-Mendoza, A., Sonké, B., Sunderland, T., Ter Steege, H., White, L.J.T., Affum-Baffoe, K., Aiba, S.I., De Almeida, E.C., De Oliveira, E.A., Alvarez-Loayza, P., Dávila, E.Á., Andrade, A., Aragão, L.E.O.C., Ashton, P., Aymard, G.A., Baker, T.R., Balinga, M., Banin, L.F., Baraloto, C., Bastin, J.F., Berry, N., Bogaert, J., Bonal, D., Bongers, F., Brienen, R., Camargo, J.L.C., Cerón, C., Moscoso, V.C., Chezeaux, E., Clark, C.J., Pacheco, Á.C., Comiskey, J.A., Valverde, F.C., Coronado, E.N.H., Dargie, G., Davies, S.J., De Canniere, C., Djuikouo, M.N., Doucet, J.L., Erwin, T.L., Espejo, J.S., Ewango, C.E.N., Fauset, S., Feldpausch, T.R., Herrera, R., Gilpin, M., Gloor, E., Hall, J.S., Harris, D.J., Hart, T.B., Kartawinata, K., Kho, L.K., Kitayama, K., Laurance, S.G.W., Laurance, W.F., Leal, M.E., Lovejoy, T., Lovett, J.C., Lukasu, F.M., Makana, J.R., Malhi, Y., Maracahipes, L., Marimon, B.S., Junior, B.H.M., Marshall, A.R., Morandi, P.S., Mukendi, J.T., Mukinzi, J., Nilus, R.,

1082 Vargas, P.N., Camacho, N.C.P., Pardo, G., Peña-Claros, M., Pétronelli, P., Pickavance,
1083 G.C., Poulsen, A.D., Poulsen, J.R., Primack, R.B., Priyadi, H., Quesada, C.A., Reitsma,
1084 J., Réjou-Méchain, M., Restrepo, Z., Rutishauser, E., Salim, K.A., Salomão, R.P.,
1085 Samsoedin, I., Sheil, D., Sierra, R., Silveira, M., Slik, J.W.F., Steel, L., Taedoumg, H.,
1086 Tan, S., Terborgh, J.W., Thomas, S.C., Toledo, M., Umunay, P.M., Gamarra, L.V.,
1087 Vieira, I.C.G., Vos, V.A., Wang, O., Willcock, S. & Zemagho, L. (2017) Diversity and
1088 carbon storage across the tropical forest biome. *Scientific Reports*, **7**, 39102.
1089 Tang, H. & Dubayah, R. (2017) Light-driven growth in Amazon evergreen forests explained
1090 by seasonal variations of vertical canopy structure. *Proceedings of the National*
1091 *Academy of Sciences of the United States of America*, **114**, 2640–2644.
1092 Thomas, R.Q., Kellner, J.R., Clark, D.B. & Peart, D.R. (2013) Low mortality in tall tropical
1093 trees. *Ecology*, **94**, 920–929.
1094 Le Toan, T., Quegan, S., Davidson, M.W.J., Balzter, H., Paillou, P., Papathanassiou, K.,
1095 Plummer, S., Rocca, F., Saatchi, S., Shugart, H. & Ulander, L. (2011) The BIOMASS
1096 mission: Mapping global forest biomass to better understand the terrestrial carbon cycle.
1097 *Remote Sensing of Environment*, **115**, 2850–2860.
1098 Vincent, G., Antin, C., Laurans, M., Heurtebize, J., Durrieu, S., Lavalley, C. & Dauzat, J.
1099 (2017) Mapping plant area index of tropical evergreen forest by airborne laser scanning.
1100 A cross-validation study using LAI2200 optical sensor. *Remote Sensing of Environment*,
1101 **198**, 254–266.
1102 Xu, L., Saatchi, S.S., Shapiro, A., Meyer, V., Ferraz, A., Yang, Y., Bastin, J.-F., Banks, N.,
1103 Boeckx, P., Verbeeck, H., Lewis, S.L., Muanza, E.T., Bongwele, E., Kayembe, F.,
1104 Mbenza, D., Kalau, La., Mukendi, F., Ilunga, F. & Ebuta, D. (2017) Spatial distribution of
1105 carbon stored in forests of the Democratic Republic of Congo. *Scientific Reports*.
1106 Zanne, A.E., Lopez-Gonzalez, G., Coomes, D.A., Ilic, J., Jansen, S., Lewis, S.L., Miller, R.B.,
1107 Swenson, N.G., Wiemann, M.C. & Chave, J. (2009) Global wood density database.
1108 *Dryad*, **235**, 33.
1109

Data accessibility

Data for plots in the CTFS network are available through the online portal at http://www.forestgeo.si.edu; in the Forestplot network at https://www.forestplots.net/ and in the TEAM network at http://www.teamnetwork.org/.

Biosketches

Jean-Francois Bastin is a Post-Doctoral Fellow of the Crowther Lab at the Institute of Integrative Biology, Department of Environmental Systems Science, ETH-Zurich. He is an ecologist and a geographer using remote sensing to study the effect of global change on terrestrial ecosystems.

Ervan Rutishauser is a Post-doctoral Fellow at Smithsonian Tropical Research Institute, broadly interested in understanding environmental resilience to natural or human-induced disturbances. He aims at providing rigorous and practical evidences to trigger a shift towards better ressources management and conservation.

Supplementary information.

Supplementary table 1. Plot, Site and PIs

Supplementary table 2. Coefficients of plot level structure prediction from the *ith* largest trees.

Supplementary figure 1. Cross-continent comparison of plot-metrics distribution averaged at the site level.

Supplementary figure 2. Lorey's Height prediction from the 20 largest trees.

Supplementary figure 3. PCA on the diameter structure and corresponding mean distribution for high contributions of axis 1 and axis 2.

Supplementary figure 4. Cross-continent comparison of the relative residuals from the prediction of plot-metrics from the 20 largest trees.

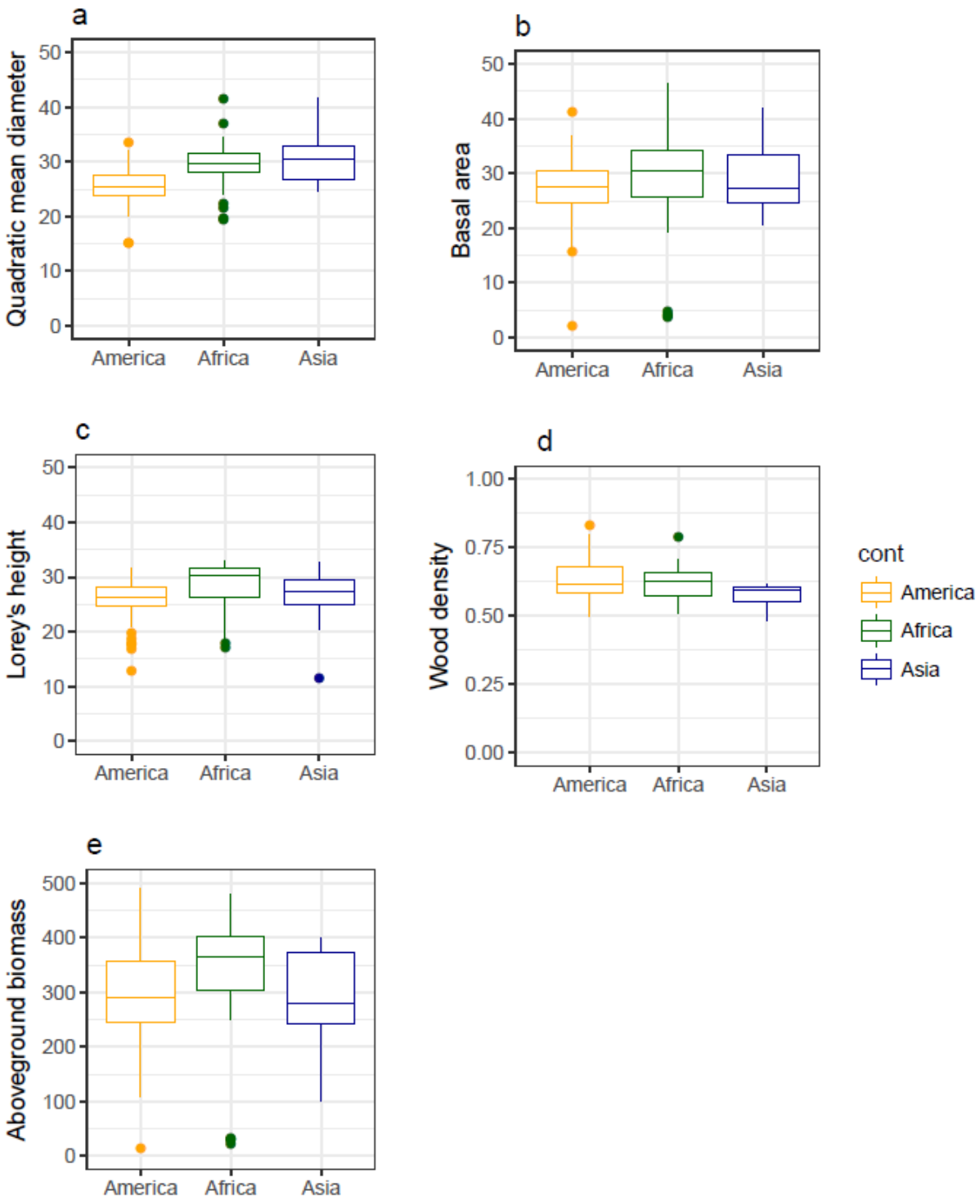

Supplementary figure 1. Cross-continent comparison of plot-metrics distribution averaged at the site level. Figures illustrates respectively the distribution of the values for the quadratic mean diameter (a), basal area (b), Lorey's height (c), wood density (d) and aboveground biomass (e).

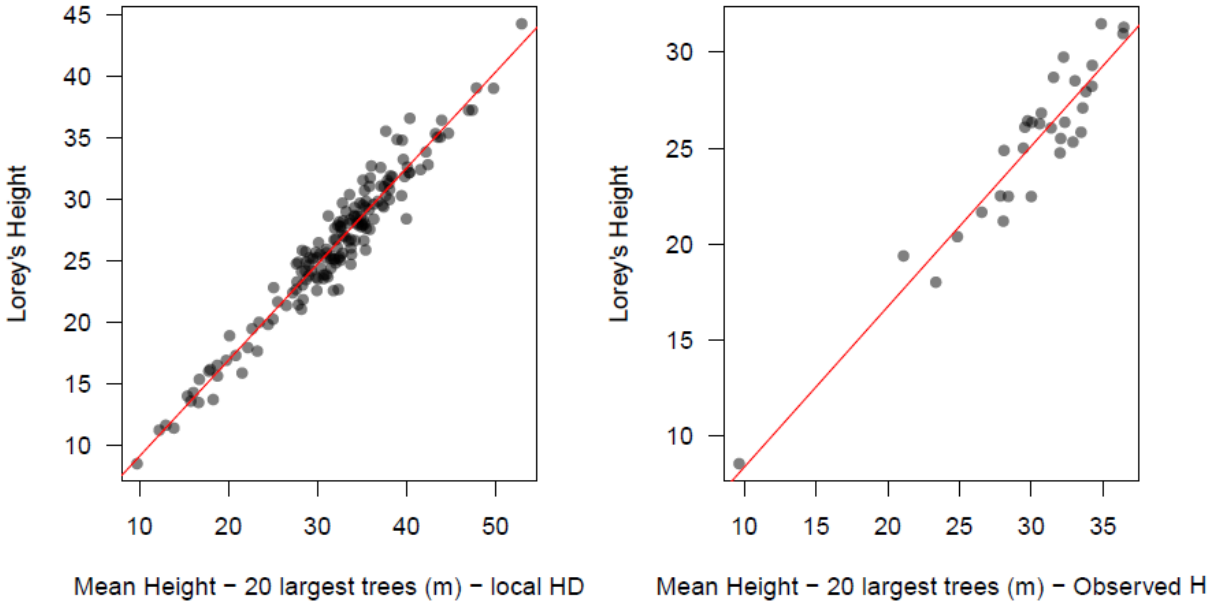

1139

1140 **Supplementary figure 2. Lorey's Height prediction from the 20 largest trees.** Figures

1141 show the results using (i) local D-H allometries for 20 sites (left subfigure) and (ii) using plots

1142 where height is measured on all trees in Malebo site in the Democratic Republic of the Congo

1143 (right subfigure).

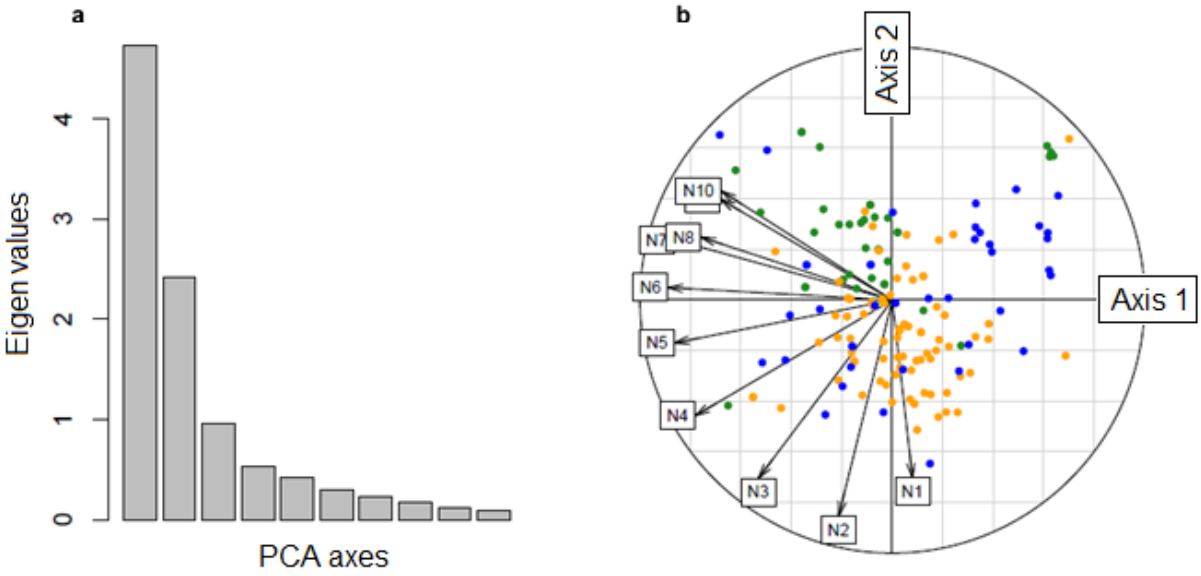

Supplementary figure 3. PCA on the diameter structure and corresponding mean distribution for high contributions of axis 1 and axis 2. (A) Illustration of top and low percentile observed for each axis, with diameter distributions represented as the relative difference with the average observed distribution.(B) Biplot with contribution to the PCA of all the diameter classes, with the respective position of each site in the space defined by axis1 and 2. Axis 1 is driven by differences in global abundance of trees and axis 2 is driven by a difference of balance between abundance of small vs. large trees. Colors represent continent, with Africa, America and Asia respectively in green, orange and blue.

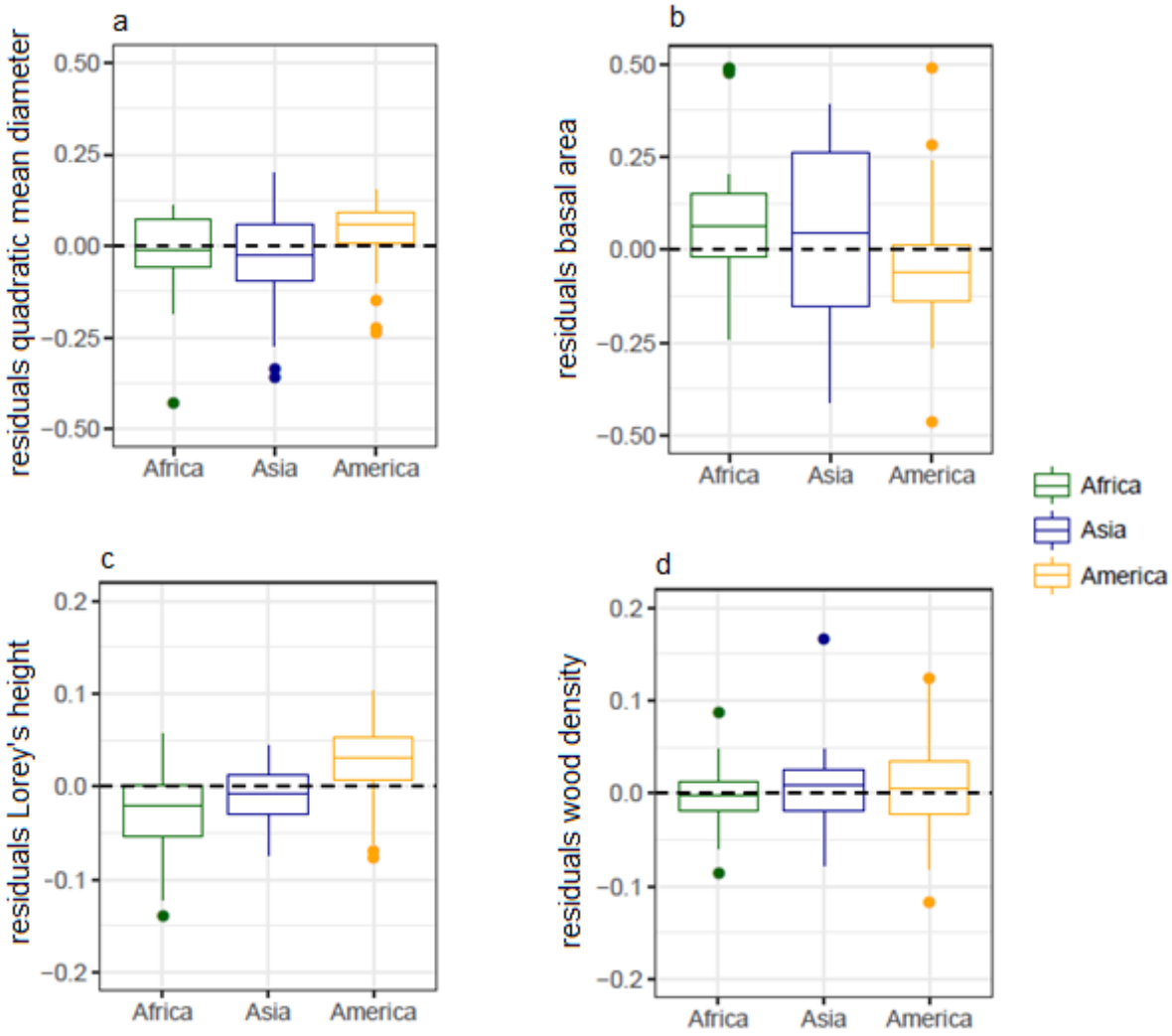

Supplementary figure 4. Cross-continent comparison of the relative residuals from the prediction of plot-metrics from the 20 largest trees. The relative residuals are generally low (<10%). Systematic small differences can however be found in America, where the quadratic mean diameter and Lorey's height tend to be slightly overestimated and the basal area slightly underestimated.